DOI: 10.1002/chem.201200713

Ligand Steric and Fluoroalkyl Substituent Effects on Enchainment Cooperativity and Stability in Bimetallic Nickel(II) Polymerization Catalysts

Michael P. Weberski, Jr., Changle Chen, Massimiliano Delferro,* and Tobin J. Marks*[a]

Abstract: The synthesis and characterization of two neutrally charged bimetallic Ni^{II} ethylene polymerization catalysts, {2,7-di-[2,6-(3,5-di-methylphenylimino)methyl]1,8-naphthalenediolato}-bis-Ni^{II}(methyl)(trimethylphosphine) [**$(CH_3)FI^2$-Ni_2**] and {2,7-di-[2,6-(3,5-ditrifluoromethyl-phenylimino)methyl]-1,8-naphthalenediolato}-bis-Ni^{II}-(methyl)(trimethyl-phosphine) [**$(CF_3)FI^2$-Ni_2**)], are reported. The diffraction-derived molecular structure of **$(CF_3)FI^2$-Ni_2** reveals a Ni···Ni distance of 5.8024(5) Å. In the presence of ethylene and $Ni(COD)_2$ or $B(C_6F_5)_3$ cocatalysts, these complexes along with their monometallic analogues [2-*tert*-butyl-6-((2,6-(3,5-dimethylphenyl)phenylimino)methyl)-phenolate]-Ni^{II}-methyl(trimethylphosphine) [**(CH_3)FI-Ni**] and [2-*tert*-butyl-6-((2,6-(3,5-ditrifluoromethyl-phenyl)phenylimino)methyl)-phenolato]-Ni^{II}-methyl-(trimethylphosphine) [**(CF_3)FI-Ni**], produce polyethylenes ranging from highly branched $M_w = 1400$ oligomers (91 methyl branches per 1000 C) to low branch density $M_w = 92\,000$ polyethylenes (7 methyl branches per 1000 C). In the bimetallic catalysts, Ni···Ni cooperative effects are evidenced by increased product polyethylene branching in ethylene homopolymerizations (~3× for **$(CF_3)FI^2$-Ni_2** vs. monometallic **(CF_3)FI-Ni**), as well as by enhanced norbornene co-monomer incorporation selectivity, with bimetallic **$(CH_3)FI^2$-Ni_2** and **$(CF_3)FI^2$-Ni_2** enchaining approximately three- and six-times more norbornene, respectively, than monometallic **(CH_3)FI-Ni** and **(CF_3)FI-Ni**. Additionally, **$(CH_3)FI^2$-Ni_2** and **$(CF_3)FI^2$-Ni_2** exhibit significantly enhanced thermal stability versus the less sterically encumbered dinickel catalyst {2,7-di-[(2,6-diisopropylphenyl)imino]-1,8-naphthalenediolato}-bis-Ni^{II}-(methyl)(trimethylphosphine). The pathway for bimetallic catalyst thermal deactivation is shown to involve an unexpected polymerization-active intermediate, {2,7-di-[2,6-(3,5-di-trifluoromethyl-phenylimino)methyl]-1-hydroxy,8-naphthalenediolato-Ni^{II}-(methyl)-(trimethylphosphine).

Keywords: bimetallic catalysts · cooperative effects · homogeneous catalysis · nickel · polymerization

Introduction

Pronounced enchainment cooperativity effects between covalently linked group 4 metal centers in binuclear CGC (constrained geometry catalyst) olefin polymerization catalysts, such as **C2-Zr_2** and **C1-Zr_2**, have been reported from this laboratory.[1] These catalysts include significantly enhanced polyethylene branching and remarkably increased co-monomer enchainment selectivity with respect to monometallic analogues **M_1** (Scheme 1).[1b,2] Note, some aspects of these processes mimic binuclear metalloenzyme cooperative effects in how substrates are selectively activated and concentrated.[3–5] The proposed pathway by which these catalysts produce novel macromolecular architectures involves

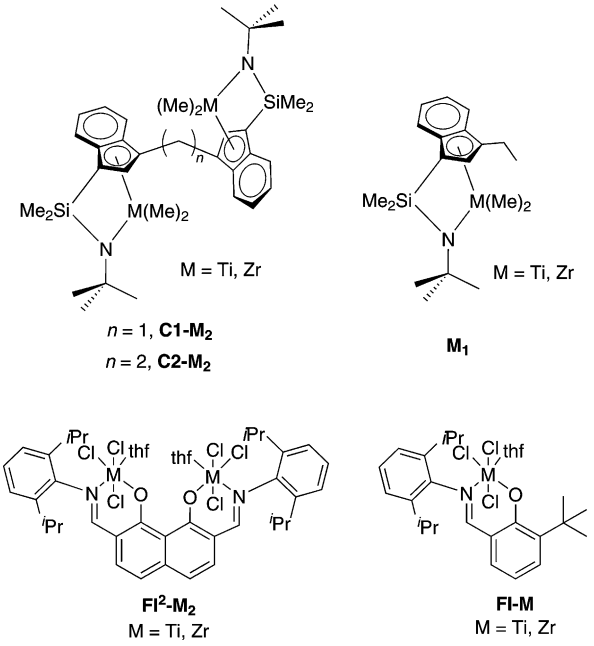

Scheme 1. Group 4 monometallic and bimetallic olefin polymerization catalysts.

[a] Dr. M. P. Weberski, Jr., Dr. C. Chen, Dr. M. Delferro, Prof. Dr. T. J. Marks
Department of Chemistry, Northwestern University
Evanston, Illinois 60208-3113 (USA)
Fax: (+1) 847 491 2990
E-mail: m-delferro@northwestern.edu
t-marks@nortwestern.edu

Supporting information for this article is available on the WWW under http://dx.doi.org/10.1002/chem.201200713: includes catalyst and polymer characterization, crystallographic data for **$(CF_3)H_2FI^2$** and **$(CF_3)FI^2$-Ni_2·0.5(C_6H_{14})**.

secondary interactions between weakly basic monomer functionalities (e.g., C–H, Ph) and the proximate active catalytic centers, as suggested by low temperature ^{1}H NMR spectroscopy[6] and DFT calculations (Figure 1).[7] In group 4 mediated polymerizations, the magnitude of these cooperative effects scales approximately inversely with metal···metal distance.[1b]

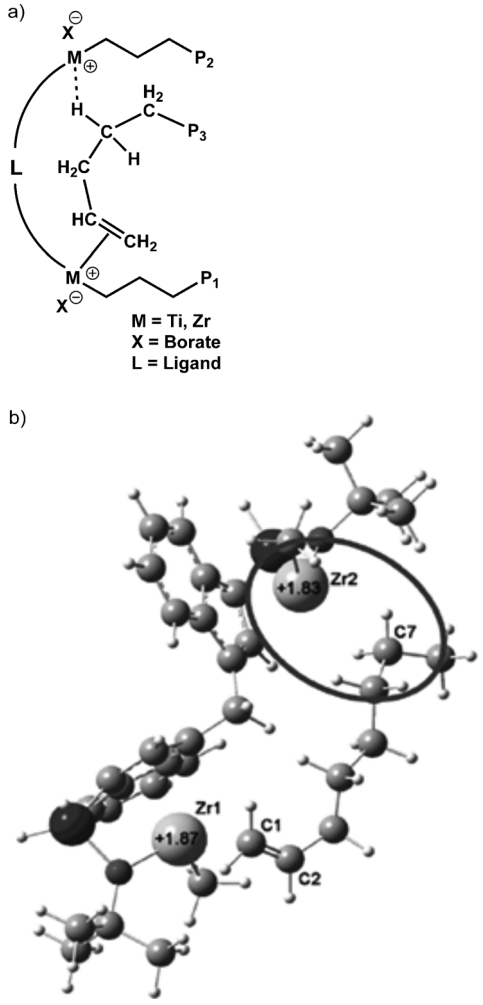

Figure 1. a) Schematic of proposed bimetallic catalyst–substrate activation/binding in ethylene-*co*-hexene polymerization catalysis mediated by binuclear catalysts **C2-M$_2$** and **C1-M$_2$**; P^1, P^2, P^3 = polymer fragment. b) DFT modeling of bimetallic 1-octene binding to the *R*,*R* diastereoisomer of the **C1-Zr$_2$** dication. The agostic interaction with a 1-octene methylene group is circled.

Recently, the scope of these cooperativity effects was extended from group 4 CGC to phenoxyiminato systems, building on the mononuclear catalysts of Grubbs[8] and Fujita.[9] Similar to the binuclear CGC catalysts, binuclear group 4 phenoxyiminato-based **FI^2-M$_2$** catalysts (M = Ti, Zr; Scheme 1) display increased α-olefin co-monomer enchainment selectivity in ethylene copolymerizations.[10] Specifically, selectivity for 1-hexene, 1-octene, and highly encumbered 1,1-disubstituted cycloalkene enchainment, as well as a marked increase in activity over the corresponding **FI-M** monometallic analogues (M = Ti, Zr; Scheme 1), is observed. Interestingly, the Ti versus Zr reactivity patterns in these bimetallic phenoxyiminato catalysts are very different from those in the CGC systems, for example, **FI^2-Zr$_2$** is a more active ethylene polymerization catalyst than is **FI^2-Ti$_2$**.[10a]

The area of group 10 olefin polymerization catalysis,[11] in particular Ni^{II} complexes,[12,13] has received much recent attention[14] since the pioneering discovery of bulky aryl-substituted cationic α-diimine Ni^{II} and Pd^{II} catalysts by Brookhart and co-workers[15] (Scheme 2). These catalysts effect the polymerization of ethylene at high rates and the copolymerization of ethylene with polar co-monomers, such as acrylates, vinyl ketones, and silyl-vinyl ethers.[14d,j, o, 15d] Detailed mechanistic studies reveal that these catalysts produce highly branched polyethylenes through sequences of rapid β-H elimination and subsequent reinsertion, that is, "chain-walking".[11i,16] Highly active, neutrally-charged Ni^{II} phenoxy-iminato ethylene polymerization catalysts reported by Grubbs[8] (Scheme 2) are tolerant toward polar solvents and are competent to enchain polar-substituted norbornenes into polyethylene backbones.

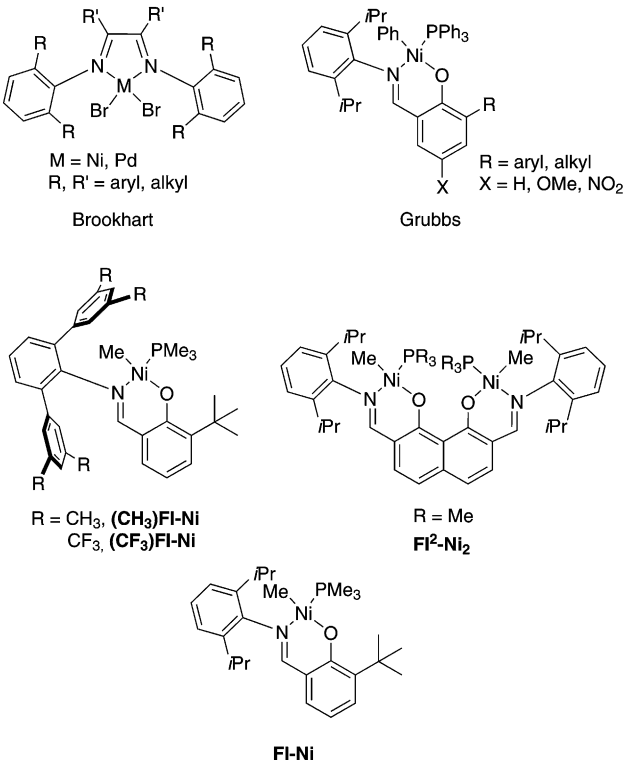

Scheme 2. Examples of Ni^{II} olefin polymerization catalysts.

We recently reported that neutrally-charged mononuclear Ni^{II} catalysts **(CH$_3$)FI-Ni** and **(CF$_3$)FI-Ni** (Scheme 2) afford markedly different product polyethylenes and at very different rates: **(CH$_3$)FI-Ni** produces densely branched oligomers with $M_w = 1.4\ kg\,mol^{-1}$, whereas in contrast, **(CF$_3$)FI-Ni** produces modestly branched polyethylenes with M_w =

92 kg mol^{-1} at 6.5-times the polymerization activity.[17] From 2D ^{19}F, ^{1}H HOESY NMR spectroscopy and molecular modeling it was argued that the remote ligand CF_3 groups can engage in C–F···H–C interactions[18] with hydrogen atoms on the β-carbon of Ni-alkyl/polymeryl groups,[9b,d,17,19] disfavoring conformers required to access the favorable *syn*-periplanar conformation preceding β-H elimination (Scheme 3). This interaction yields catalysts that produce dramatically higher M_w polyethylenes with significantly less branching than the non-fluorinated analogues.

In related work, bimetallic nickel(II) catalyst **FI^2-Ni$_2$** (Scheme 2) was shown[6,20] to increase polyethylene branch formation as well as co-monomer enchainment selectivity, including that of polar norbornenes and acrylates, over that of monometallic **FI-Ni**. Nevertheless, **FI^2-Ni$_2$** undergoes significant thermal deactivation, forming a catalytically inactive bis-ligated species on exposure to temperatures above 40 °C (Scheme 4).[6,20]

In an effort to better understand ligation effects on cooperativity and stability in this system, we report here the synthesis and properties of new bimetallic Ni^{II} phenoxyiminato-based catalysts **(CH$_3$)FI^2-Ni$_2$** and **(CF$_3$)FI^2-Ni$_2$** (Scheme 5) that contain sterically encumbered and fluorocarbon-substituted polyaryl substituents. Among the interesting findings, it is found that these bulky substituents significantly suppress catalyst deactivation through the redistribution pathway shown in Scheme 4. Details of this deactivation pathway are scrutinized here, and an unexpected monometallic polymerization-active intermediate **(CF$_3$)FI^2-Ni(OH)** is identified and shown to contribute significantly to polyethylene production at 50 °C. All evidence argues that the predominant deactivation pathway for bimetallic **(CH$_3$)FI^2-Ni$_2$** and **(CF$_3$)FI^2-Ni$_2$** does not involve ligand redistribution, but rather reductive elimination of an Ni–H functionality to yield the corresponding protonated ligand and Ni^0. Furthermore, we report that Ni(COD)$_2$ functions here as a "non-innocent" co-catalyst and is also capable of mediating ethylene polymerization in the presence of the free ligand liberated during **(CH$_3$)FI^2-Ni$_2$**, **(CF$_3$)FI^2-Ni$_2$** and **(CF$_3$)FI^2-Ni(OH)** thermolysis. Finally, marked catalyst center···catalyst center cooperative effects are observed in ethylene-*co*-norbornene polymerizations, with **(CH$_3$)FI^2-Ni$_2$** and **(CF$_3$)FI^2-Ni$_2$** displaying significantly greater norbornene enchainment selectivity than their monometallic counterparts.

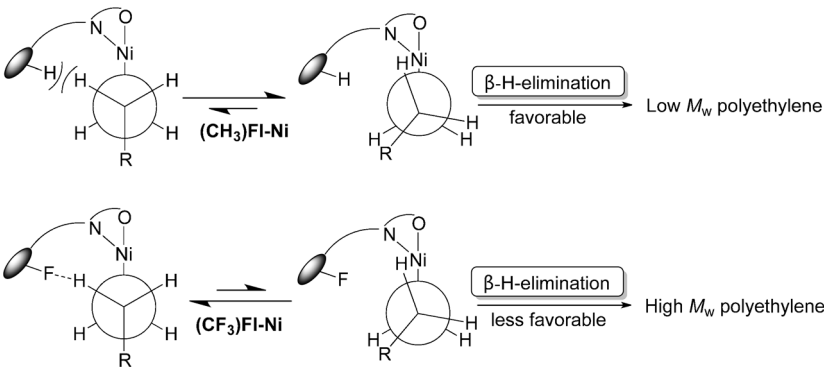

Scheme 3. Newman projections illustrating how (ligand)F···H(alkyl) interactions disfavor the *syn*-periplanar conformation, which facilitates β-H elimination.

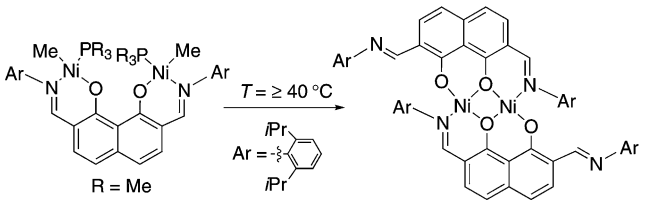

Scheme 4. Proposed thermal deactivation pathway of bimetallic Ni^{II} catalyst **FI^2-Ni$_2$**.

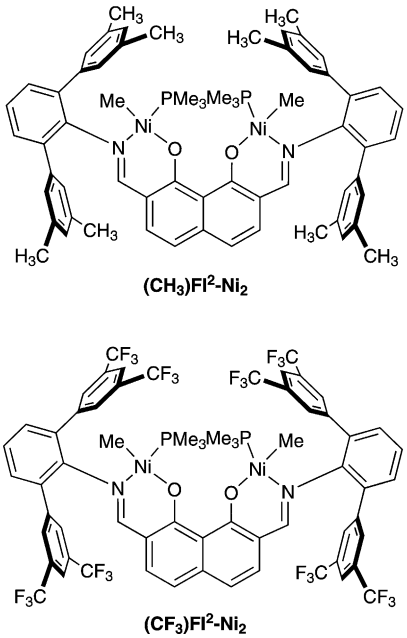

Scheme 5. Bimetallic Ni^{II} catalysts investigated in this study.

Results

A principal goal of this study was to investigate ligand substituent steric and fluorocarbon effects on the polymerization cooperativity and chain transfer characteristics as well as thermal stability of bimetallic Ni^{II} ethylene polymerization catalysts. Sterically encumbered ligand terphenyl substituents are introduced with the aim of possibly suppressing intermolecular redistribution processes (Scheme 4) and assessing the effects of bulky and fluorocarbon substituents (Scheme 3). The ethylene polymerization behavior of the bimetallic catalysts **(CH$_3$)FI^2-Ni$_2$** and **(CF$_3$)FI^2-Ni$_2$**, as well as their corresponding monome-

tallic analogues **(CH_3)FI-Ni** and **(CF_3)FI-Ni**,[17] are first investigated. Ethylene-*co*-norbornene polymerizations are also conducted to investigate the nature of metal center···· metal center cooperativity that these catalysts might display. Specific attention is focused on the deactivation pathways these bimetallic ethylene polymerization catalysts traverse at elevated temperatures. A polymerization active intermediate, **$(CF_3)FI^2$-Ni(OH)**, is identified in the deactivation pathway of bimetallic catalyst **$(CF_3)FI^2$-Ni_2**. In 50 °C ethylene polymerizations when using catalyst **$(CF_3)FI^2$-Ni_2**, **$(CF_3)FI^2$-Ni(OH)** accounts for a significant fraction of the polyethylene production.

Catalyst synthesis: The ligand reagent 2,7-diformyl-1,8-naphthalenediol (**1**) was obtained by a previously published synthesis route,[10,21] whereas the hindered terphenyl amines were prepared by using Suzuki cross-coupling procedures.[22] The bimetallic ligands **$(CH_3)H_2FI^2$** and **$(CF_3)H_2FI^2$** were synthesized through condensation reactions between **1** and the appropriate terphenyl amine (Scheme 6). The condensations were carried out by using a Dean–Stark apparatus with a catalytic amount of formic or *p*-toluenesulfonic acid, and proceeded slowly, presumably because of the steric encumbrance of the terphenyl amine. The reactions proceed via isolable half-condensation products (**2**),[23] which react with a second equivalent of amine, affording the product over the course of 3 and 7 days for **$(CF_3)H_2FI^2$** and **$(CH_3)H_2FI^2$**, respectively, in refluxing toluene. Both ligands are purified by recrystallization from toluene/methanol. ^{1}H NMR analysis of **$(CH_3)H_2FI^2$** and **$(CF_3)H_2FI^2$** solutions left standing in air for several days evidence significant hydrolytic decomposition, yielding the corresponding half-condensation product and 1 equiv free amine.[24] Similar to the previously reported phenoxyiminato bimetallic ligand **H_2FI^2**,[10] both **$(CH_3)H_2FI^2$** and **$(CF_3)H_2FI^2$** undergo dynamic structural rearrangement processes (keto-amino/enol-imine tautomerism, Figure 2)[25] in solution that are sufficiently slow on the NMR timescale[26] to resolve a single dissymmetric species below about

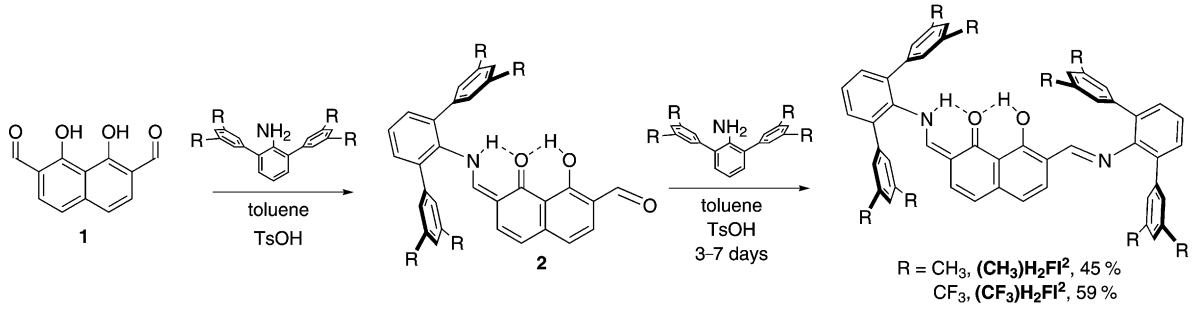

Scheme 6. Synthesis of bimetallic ligands **$(CH_3)H_2FI^2$** and **$(CF_3)H_2FI^2$**.

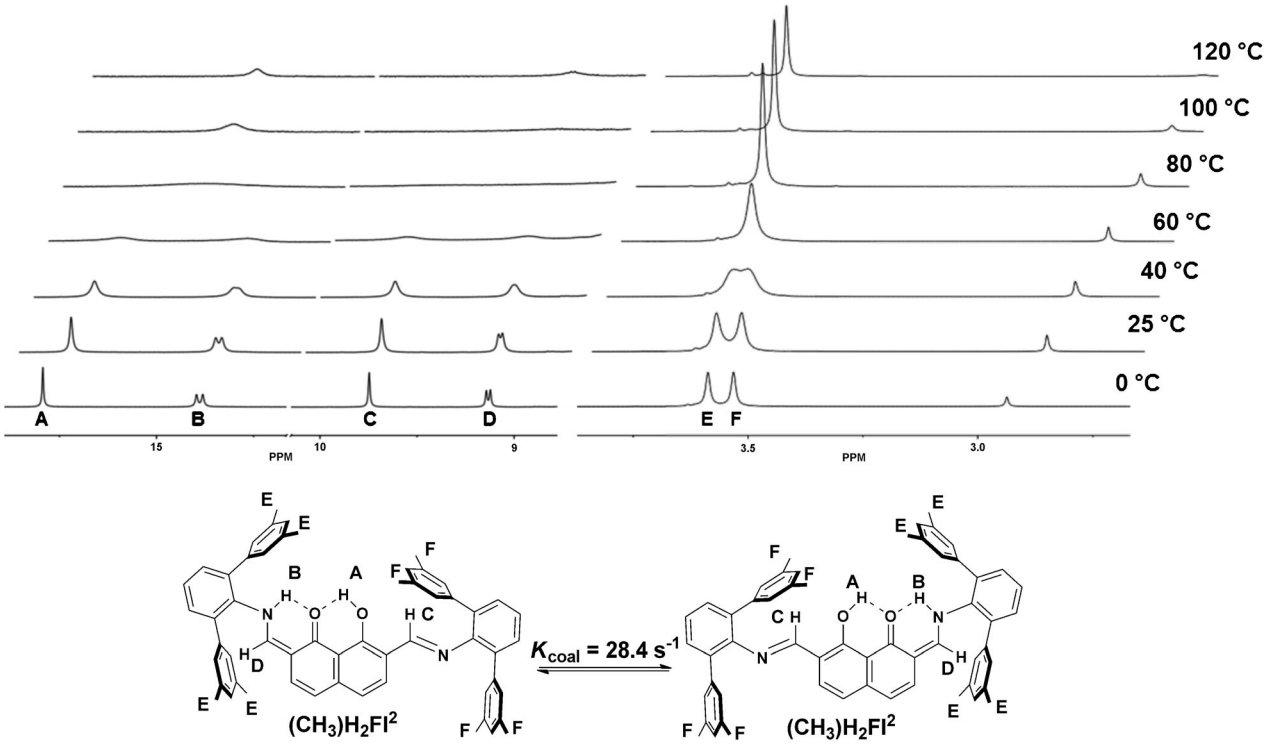

Figure 2. Variable-temperature ^{1}H NMR (400 MHz, 1,1,2,2,-tetrachloroethane) stack plot spectra for the keto-amine tautomerism in **$(CH_3)H_2FI^2$** (*T* coalescence ≈ 80 °C).

80°, with a rate constant (k_{coal}) of approximately 28 s^{-1} and $\Delta G^{\ddagger}$ (353 K) of about 18 kcal mol^{-1}, typical of such tautomerisms.[27] The proposed solution structure is consistent with the solid-state molecular structure (see below), and the spectral coalescence temperature is not significantly affected by the terphenyl ring substituents.

The disodium salts of **$(CH_3)H_2FI^2$** and **$(CF_3)H_2FI_2$** are prepared by stirring the free ligands with excess NaH in dry THF for 2 days.[28] The bimetallic catalysts **$(CH_3)FI^2$-Ni_2** and **$(CF_3)FI_2$-Ni_2** are then prepared by treating the ligand disodium salts with 2 equiv *trans*-NiClMe-$(PMe_3)_2$[29] in benzene and toluene, respectively (Scheme 7). The **$(CH_3)FI^2$-Ni_2** synthesis proceeds cleanly on stirring in benzene at room temperature, overnight; however, the use of these conditions for the **$(CF_3)FI^2$-Ni_2** synthesis leads to the isolation of small amounts of $NiCl_2(PMe_3)_2$[29] and other unidentified byproducts. These can be minimized by slowly warming the reaction mixture from −78 to 25 °C over a period of 7 h in toluene. Monometallic catalysts **$(CH_3)FI$-Ni** and **$(CF_3)FI$-Ni** were prepared according to literature procedures.[17]

In investigating any reactivity that bimetallic ligand **$(CF_3)H_2FI^2$** might exhibit toward bimetallic Ni^{II} complex

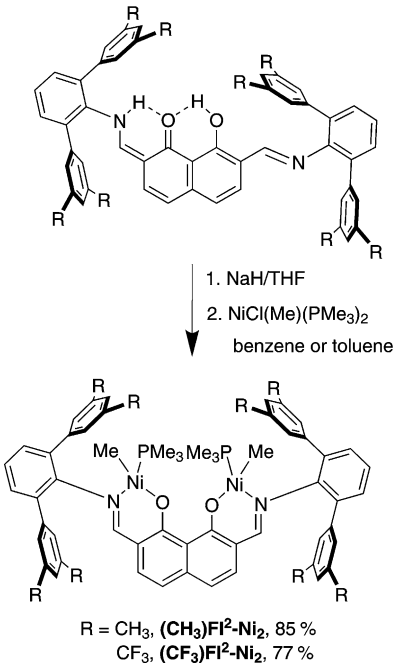

Scheme 7. Synthesis of bimetallic catalysts **$(CH_3)FI^2$-Ni_2** and **$(CF_3)FI^2$-Ni_2**.

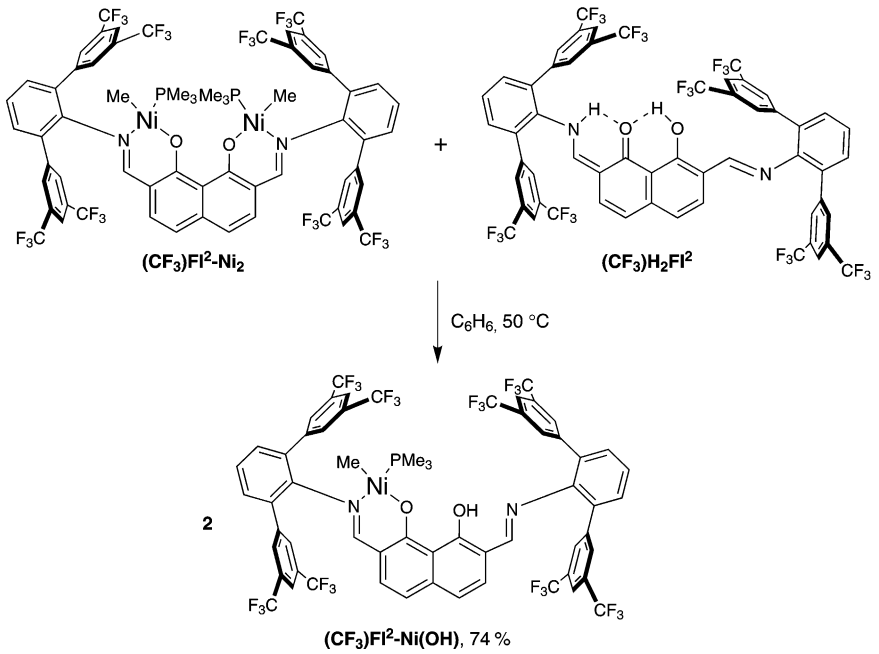

Scheme 8. Comproportionation reaction of **$(CF_3)FI^2$-Ni_2** and **$(CF_3)H_2FI^2$** to afford **$(CF_3)FI^2$-Ni(OH)**.

$(CF_3)FI^2$-Ni_2, a comproportionation reaction was discovered that cleanly affords complex **$(CF_3)FI^2$-Ni(OH)** in high yield (Scheme 8). Complex **$(CF_3)FI^2$-Ni(OH)** is prepared by stirring equimolar amounts of **$(CF_3)H_2FI^2$** and **$(CF_3)FI^2$-Ni_2** at 50 °C in benzene, overnight. Removal of the volatiles affords spectroscopically pure **$(CF_3)FI^2$-Ni(OH)**.

Molecular structure of binucleating ligand $(CF_3)H_2FI^2$: Single crystals of ligand **$(CF_3)H_2FI^2$** were grown by slow evaporation of a $CDCl_3$ solution. A displacement ellipsoid plot of **$(CF_3)H_2FI^2$** is shown in Figure 3. Selected bond distances and angles are included in the Figure caption. **$(CF_3)H_2FI^2$** crystallizes in triclinic space group $P\bar{1}$ with two molecules in the asymmetric unit. The structure displays two intramolecular hydrogen bonds (the H atoms H1 and H2 were found in the electron density difference map) between O1−H1···O2 (1.65(5) Å), and N2−H2···O2 (1.92(4) Å), which form two six-membered pseudo-rings.[30] The distance between phenol O2 atom and imine N2 atom (2.56(2) Å) is shorter than the average distance found in the Cambridge Crystallographic Data Centre (CCDC) (2.67(1) Å), whereas the distance between phenol atom O1 and phenol atom O2 (2.52(3) Å) is negligibly different from the average distance (2.55(2) Å) found in the CCDC.[31] The solid-state structure of **$(CF_3)H_2FI^2$** displays a dissymmetric orientation and tautomerization is evidenced by elongation of the C1−O1 and C34−N2 distances. The tautomerization and hydrogen bonding present in **$(CF_3)H_2FI^2$** are similar to that previously reported in the less sterically encumbered bimetallic ligand, **H_2FI^2**.[10] The crystal packing is dominated by intermolecular C−H···F−C hydrogen bonds[18a,c–e] at distances ranging from 2.49–2.52 Å; these C−H···F distances are typical of interactions of this type.[18a,c–e]

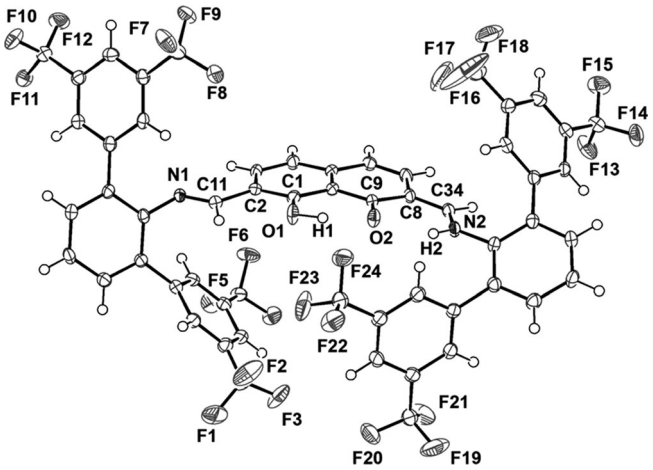

Figure 3. ORTEP plot of the molecular structure of dinucleating ligand **$(CF_3)H_2FI^2$**. Thermal ellipsoids are drawn at the 50% probability level. Hydrogen atoms are drawn as arbitrarily small spheres. Selected bond distances (Å) and angles (°): C1–O1 1.343(3); C9–O2 1.282(3); C2–C11 1.460(4); C8–C34 1.390(4); C34–N2 1.323(4); C11–N1 1.278(4); ∢C2–C11–N1 122.2(3); ∢C8–C34–N2 123.2(3); ∢C1–C2–C11–N1 178.9(3); ∢C9–C8–C34–N2 –2.1(5).

Molecular structure of binuclear precatalyst $(CF_3)FI^2$-Ni_2: Single crystals of **$(CF_3)FI^2$-Ni_2** were grown by slow evaporation of an *n*-hexane solution under N_2. A displacement ellipsoid plot of **$(CF_3)FI^2$-Ni_2** is shown in Figure 4. Selected bond distances and angles are included in the Figure caption. Complex **$(CF_3)FI^2$-Ni_2** crystallizes with one-half of a molecule of *n*-hexane in the asymmetric unit ($Z=2$) in space group $P\bar{1}$. The configuration about each Ni in **$(CF_3)FI^2$-Ni_2** shows the trimethylphosphine ligands to be positioned *trans* to the imine functionalities; both Ni atoms in **$(CF_3)FI^2$-Ni_2** adopt a distorted square-planar coordination geometry. Around Ni1, atoms P1 and C1 are displaced +0.500(2) and −0.324(3) Å, respectively, from the Ni1/O1/N1 mean plane; around Ni2, atoms P2 and C2 are displaced −0.559(2) and +0.279(3) Å, respectively, from the Ni2/O2/N2 mean plane. Significant twisting of the Ni square planes is also observed in **$(CF_3)FI^2$-Ni_2** (Figure 5). Around Ni1, the plane containing the naphthalene backbone (PL 1 = C9–C18) and the plane containing Ni1 and the atoms directly bound to Ni1 (PL 2 = Ni1/O1/N1/C1/P1) display a dihedral angle of 19.11(5)°. The dihedral angle between PL 1 and the mean plane defined by Ni2 and the atoms directly bound to Ni2 (PL 3 = Ni2/O2/N2/C2/P2) is found to be 37.48(4)°, whereas the dihedral angle between the two planes containing Ni1 and Ni2 (PL2 and PL3, respectively) is 53.69(4)°.

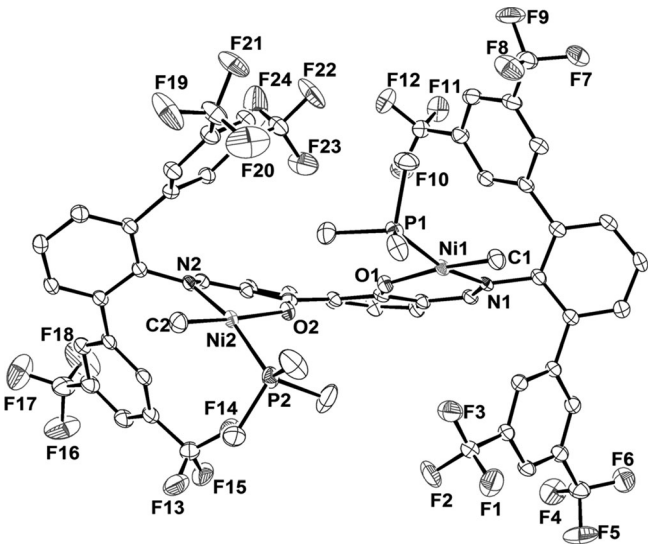

Figure 4. ORTEP plot of binuclear precatalyst **$(CF_3)FI^2$-Ni_2**. Thermal ellipsoids are drawn at the 50% probability level. H atoms and solvent molecules are omitted for clarity. Selected bond distances (Å) and angles (°): Ni1···Ni2 5.8024(5); Ni1–C1 1.941(2); Ni2–C2 1.943(2); Ni1–P1 2.1528(7); Ni2–P2 2.1391(7); Ni1–N1 1.929(2); Ni2–N2 1.944(2); Ni1–O1 1.896(2); Ni2–O2 1.899(2); ∢N1–Ni1–C1 94.60(9); ∢N2–Ni2–C2 94.23(9); ∢C1–Ni1–P1 85.17(8); ∢C2–Ni2–P2 86.84(7); ∢P1–Ni1–O1 89.53(5); ∢P2–Ni2–O2 89.49(5); ∢O1–Ni1–N1 93.19(7); ∢O2–Ni2–N2 91.83(7); ∢N1–Ni1–P1 166.31(6); ∢N2–Ni2–P2 164.81(6); ∢O1–Ni1–C1 167.61(9); ∢O2–Ni2–C2 169.76(9).

Despite the distorted square-planar geometry in the solid state, **$(CF_3)FI^2$-Ni_2** and all other catalysts reported evidence diamagnetic NMR chemical shifts in solution. The Ni–ligand bond metrics ($Ni–O_{phenol}$, $Ni–N_{imine}$, $Ni–C_{methyl}$, $Ni–P_{phosphine}$, $C=N_{imine}$, $C–O_{phenol}$, Figure 4, caption)[32] are very similar in each Ni center in **$(CF_3)FI^2$-Ni_2**, and are also very similar to the previously reported structure of monometallic

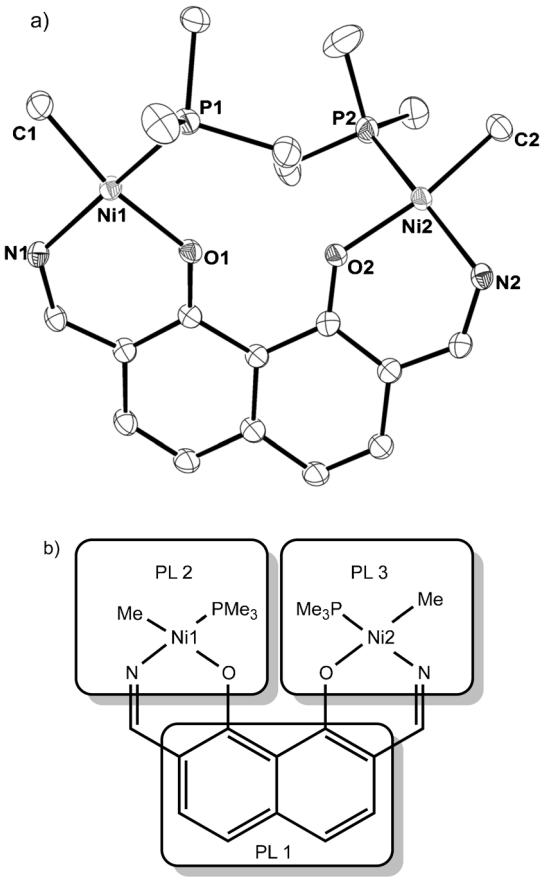

Figure 5. a) View of the **$(CF_3)FI^2$-Ni_2** molecular core with H atoms, solvent molecules, and terphenyl groups omitted for clarity. b) Plane numbering scheme for the core structure of binuclear complex **$(CF_3)FI^2$-Ni_2**.

catalyst **(CF_3)FI-Ni**,[17] and are within the distance range typical of square-planar salicylaldiminato Ni^{II} complexes.[32] In addition, these negligible differences in lengths and angles between **$(CF_3)FI^2$-Ni_2** and the salicylaldiminato Ni^{II} complex family indicate that the electron-withdrawing groups CF_3 do not significantly alter the electronic structure near the Ni center through inductive effects, however, weak fluorocarbon ligand–polymer product interactions can affect the course of ethylene polymerization (Scheme 3).[17] As expected, the crystal packing of **$(CF_3)FI^2$-Ni_2** is dominated by intermolecular aromatic C–H···F–C hydrogen bonding[18a,c–e] at distances ranging from 2.51–2.52 Å. The Ni1···Ni2 distance observed in **$(CF_3)FI^2$-Ni_2** is 5.8024(5) Å, one of the shortest Ni···Ni distances reported to date in bimetallic neutrally charged Ni^{II} catalysts,[1a,6,14k,20,33] However, this is far longer than the sum of Ni atomic van der Waals radii (3.26 Å)[34] and indicates no significant chemical interaction. Note that this value is significantly smaller than in previously reported CGC-based bimetallic catalysts **C1-Zr_2** and **C2-Zr_2** that have Zr···Zr distances of 7.392(3) and 8.671(3) Å (Scheme 1), respectively.[2e]

Ethylene homopolymerization experiments: Complexes **$(CH_3)FI^2$-Ni_2**, **$(CF_3)FI^2$-Ni_2**, **(CH_3)FI-Ni**, **(CF_3)FI-Ni**, and **$(CF_3)FI^2$-Ni(OH)** are found to be active ethylene polymerization catalysts in the presence of $Ni(COD)_2$ as a phosphine scavenger/co-catalyst; relevant data are collected in Tables 1 and 2. In the absence of co-catalyst, negligible polyethylene is obtained with the catalysts reported here. Typical ethylene homopolymerization experiments were conducted with catalyst (5 μmol) in toluene (50 mL) under a continuous ethylene pressure (8.0 atm) for 10 min by using conditions minimizing mass transport and exotherm effects.[1b,2d–g] The polymeric products were characterized by ^1H and ^{13}C NMR spectroscopy, and molecular weight by GPC with viscometry/refractive index detection versus a polystyrene standard. Polyethylene branch numbers were quantified by ^1H NMR spectroscopy.[33a,d,e,35]

Table 1. Ethylene polymerization data for experiments at room temperature.[a]

Entry	Catalyst	Polymer yield [g]	M_w ($\times 10^3$)[b]	PDI[b]	Total Me per 1000 C[c]	Act.[d]
1	**(CF_3)FI-Ni**[e]	1.661	92.0	3.0	7	250
2	**$(CF_3)FI^2$-Ni_2**	0.280	25	2.4	40	21
3	**(CH_3)FI-Ni**[e]	0.253	1.4	1.1	88	91
4	**$(CH_3)FI^2$-Ni_2**	0.120	3.8	2.0	91	9
5	**$(CF_3)FI^2$-Ni(OH)**	0.546	11	2.3	44	82

[a] All polymerizations carried out under constant 8.0 atm ethylene pressure with 5.0 μmol catalyst and 2.0 equiv $Ni(COD)_2$/Ni for 10 min in 50 mL toluene. Entries performed in duplicate. [b] From GPC versus polystyrene standards in (g mol^{-1}). [c] By ^1H NMR assay. [d] kg polymer mol^{-1}[Ni] h^{-1} atm^{-1}. [e] Data from ref. [17].

Table 2. Ethylene polymerization data for experiments at 50 °C.[a]

Entry	Catalyst	Polymer yield [g]	M_w ($\times 10^3$)[b]	PDI[b]	Total Me per 1000 C[c]	Act.[d]
1	**(CF_3)FI-Ni**[e]	3.042	7.9	2.2	40	460
2	**$(CF_3)FI^2$-Ni_2**	0.293	11	2.9	47	22
3	**$(CF_3)FI^2$-Ni_2**[f]	0.640	5.1	1.8	45	48
4	**$(CF_3)FI^2$-Ni(OH)**	3.040	6.4	1.8	63	456
5	**$(CF_3)FI^2$-Ni(OH)**[g]	0.515	6.9	2.0	57	193
6	**(CH_3)FI-Ni**[e]	0.490	1.7	1.5	99	7
7	**$(CH_3)FI^2$-Ni_2**	0.360	1.8	1.7	98	27
8	**$Ni(COD)_2 + (CF_3)H_2FI^2$**[h]	0.006	880/6.1[i]	6.2/1.8[i]	65	0.03

[a] All polymerizations carried out under constant 8.0 atm ethylene pressure with 5.0 μmol catalyst and 2.0 equiv $Ni(COD)_2$/Ni for 10 min in 50 mL toluene. Entries performed in duplicate. [b] From GPC versus polystyrene standards in (g mol^{-1}). [c] By ^1H NMR assay. [d] kg polymer mol^{-1}[Ni] h^{-1} atm^{-1}. [e] Data from ref. [17]. [f] Polymerization carried out under constant 8.0 atm ethylene pressure with 5.0 μmol catalyst and 1 equiv $B(C_6F_5)_3$/Ni for 10 min in 50 mL toluene. [g] Polymerizations carried out under constant 8.0 atm ethylene pressure with 0.5 μmol catalyst and 2.0 equiv $Ni(COD)_2$/Ni for 40 min in 50 mL toluene. [h] Polymerizations carried out with 40 μmol $Ni(COD)_2$ and 10 μmol **$(CF_3)H_2FI^2$** for 40 min in 25 mL toluene at 8.0 atm ethylene pressure. [i] GPC trace exhibits bimodal molecular weight distribution.

At room temperature, bimetallic catalysts **$(CF_3)FI^2$-Ni_2** and **$(CH_3)FI^2$-Ni_2** display ethylene polymerization activities (21 and 9 kg polymer mol^{-1}[Ni] h^{-1} atm^{-1}, respectively; Table 1, entries 2 and 4) similar to that previously reported for **FI^2-Ni_2** (7.1 kg polymer mol^{-1}[Ni] h^{-1} atm^{-1}).[20] However, ethylene polymerizations mediated by monometallic **(CH_3)FI-Ni** and **(CF_3)FI-Ni** are significantly more rapid[17] than in the case of the bimetallic catalysts. The microstructures of the polyethylenes produced by these catalysts vary greatly depending on the ligand terphenyl substitution. Thus, the polyethylenes produced by both methylterphenyl catalysts [**(CH_3)FI-Ni** and **$(CH_3)FI^2$-Ni_2**] are low molecular weight, highly branched, grease-like materials (e.g., M_w = 1400; PDI = 1.1 for **(CH_3)FI-Ni**; M_w = 3800; PDI = 2.0 for **$(CH_3)FI^2$-Ni_2**). In marked contrast, CF_3-substituted catalysts **(CF_3)FI-Ni** and **$(CF_3)FI^2$-Ni_2** produce *far higher* molecular weight polyethylenes (e.g., M_w = 92000; PDI = 2.4 for **(CF_3)FI-Ni**) with appreciably less branching versus **$(CH_3)FI^2$-Ni_2** and **(CH_3)FI-Ni**.

Monometallic **$(CF_3)FI^2$-Ni(OH)**, when activated with $Ni(COD)_2$, is an active ethylene polymerization catalyst at room temperature (Table 1, entry 5) and at 50 °C (Table 2, entries 4 and 5). At room temperature, **$(CF_3)FI^2$-Ni(OH)** exhibits four-times the activity and produces a significantly lower M_w product polyethylene than bimetallic **$(CF_3)FI^2$-Ni_2**. At 50 °C, the reactivity trends of these catalysts are similar, with **$(CF_3)FI^2$-Ni(OH)** displaying 20.7-times greater activity than bimetallic **$(CF_3)FI^2$-Ni_2**, and producing bimodal polyethylenes with a high M_w shoulder (entry 4; Figure S22 in the Supporting Information). Due to the high polymerization activity of **$(CF_3)FI^2$-Ni(OH)** relative to **$(CF_3)FI^2$-Ni_2**, and in order to minimize mass transport and exotherm effects,[1b,2d–g] polymerizations with ten-times lower catalyst loading (entry 5, 0.5 μmole) were also used. In the present study minimizing exotherms was critical since temperature has a large influence on polymer M_w, and the polymer M_w

was used to probe the mechanism of bimetallic catalyst decomposition (vide infra). Under these lower concentration conditions, catalyst **$(CF_3)FI^2$-Ni(OH)** displays 2.3-times lower activity than in the previous experiment, but produces a monomodal polyethylene. The nature of the polyethylenes obtained from **$(CF_3)FI^2$-Ni(OH)** relative to bimetallic **$(CF_3)FI^2$-Ni_2** have significant implications for the deactivation pathways of the bimetallic catalysts (vide infra). It will be shown later that **$(CF_3)FI^2$-Ni(OH)** is the predominant catalytically-active deactivation product of bimetallic **$(CF_3)FI^2$-Ni_2**.

All of the present terphenyl-substituted catalysts display appreciable ethylene polymerization activity at 50 °C (Table 2). In all cases, polyethylene molecular weights are significantly depressed and branch densities increased compared to room temperature polymerizations, except for **$(CH_3)FI^2$-Ni_2**, for which the M_w and branch density remain nearly the same as in the room temperature polymerization.

Catalyst thermal stability studies of the present bimetallic catalysts reveal that both **$(CH_3)FI^2$-Ni_2** and **$(CF_3)FI^2$-Ni_2** exhibit falling ethylene polymerization activity over time (Table 3, Figure 6), with catalyst **$(CF_3)FI^2$-Ni_2** exhibiting greater stability at 50 °C than **$(CH_3)FI^2$-Ni_2**. The polyethylenes produced by bimetallic catalysts **$(CH_3)FI^2$-Ni_2** and **$(CF_3)FI^2$-Ni_2** at 50 °C show bimodal GPC traces that can be attributed to the formation of catalytically competent deactivation products (vide infra).

Table 3. Ethylene polymerization data as a function of polymerization time at 50 °C.[a]

Catalyst	Time [min]	Polymer yield [g]	Activity[b]
$(CH_3)FI^2$-Ni_2	10	0.360	27
$(CF_3)FI^2$-Ni_2	10	0.293	22
$(CH_3)FI^2$-Ni_2	20	0.406	15
$(CF_3)FI^2$-Ni_2	20	0.506	19
$(CH_3)FI^2$-Ni_2	40	0.533	10
$(CF_3)FI^2$-Ni_2	40	0.693	13
$(CH_3)FI^2$-Ni_2	60	0.546	6.8
$(CF_3)FI^2$-Ni_2	60	0.799	10
$(CH_3)FI^2$-Ni_2	90	0.545	4.5
$(CF_3)FI^2$-Ni_2	90	1.077	9

[a] Polymerizations were out in 50 mL toluene under constant 8.0 atm ethylene pressure at 50 °C with 5.0 μmol catalyst and with 2.0 equiv Ni(COD)$_2$/Ni. [b] kg polyethylene mol^{-1}[Ni] h^{-1} atm^{-1}.

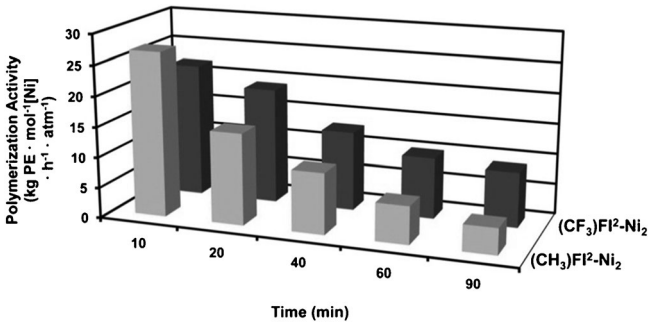

Figure 6. Temporal characteristics of **$(CH_3)FI^2$-Ni_2** and **$(CF_3)FI^2$-Ni_2** polymerization activity at 50 °C.

Similarly, when 25 °C polymerizations with the use of **$(CH_3)FI^2$-Ni_2** and **$(CF_3)FI^2$-Ni_2** are allowed to continue for 2 h, GPC analysis shows that higher M_w polyethylene begins to form.[36] In contrast, 25 °C polymerizations when using bimetallic catalysts **$(CH_3)FI^2$-Ni_2** and **$(CF_3)FI^2$-Ni_2** produce monomodal polyethylene when the polymerization time is 40 min. Investigations of the catalyst deactivation pathway will be discussed below.

To better understand the role of the co-catalyst in these polymerizations, ethylene polymerizations were conducted at 50 °C by using $B(C_6F_5)_3$ in place of Ni(COD)$_2$ as the co-catalyst and **$(CF_3)FI^2$-Ni_2** as the catalyst (Table 2). Polymerizations with $B(C_6F_5)_3$ as co-catalyst are 2.2-times more active than analogous Ni(COD)$_2$ co-catalyzed polymerizations, albeit with a significant decrease in product M_w (5.1 vs. 11 K). Additionally, the $B(C_6F_5)_3$ co-catalyzed polymerizations produce monomodal polyethylenes, whereas Ni(COD)$_2$ co-catalyzed polymerizations produce bimodal polyethylenes at 50 °C. Interestingly, it is found that Ni(COD)$_2$ functions as a "non-innocent" co-catalyst. In the presence of free ligand [**$(CF_3)H_2FI^2$**], Ni(COD)$_2$ is capable of polyethylene production at 50 °C (Table 2) with low activity. The polyethylene produced by the combination of Ni(COD)$_2$ and **$(CF_3)H_2FI_2$** is bimodal, displaying two very different product polyethylene M_w values, 880 and 6.1 K. It will be shown that during the deactivation of the bimetallic catalysts reported here, free ligand is liberated. The Ni(COD)$_2$ co-catalyst (typically used in excess) can then react with the free ligand and contribute to polyethylene production at 50 °C.

Ethylene-*co*-norbornene polymerization experiments: Ethylene + norbornene copolymerizations were carried out by using catalysts **$(CH_3)FI^2$-Ni_2**, **$(CF_3)FI^2$-Ni_2**, **$(CH_3)FI$-Ni**, and **$(CF_3)FI$-Ni** with Ni(COD)$_2$ as co-catalyst. Data are summarized in Table 4, with the norbornene content of the copolymers determined by ^{13}C NMR spectroscopy.[35c,37] Bimetallic catalyst **$(CH_3)FI^2$-Ni_2** introduces approximately three-times

Table 4. Ethylene-*co*-norbornene copolymerization data.[a]

Catalyst	Polymer yield [g]	M_w ($\times 10^3$)[c]	PDI[c]	Total Me per 1000 C[d]	Act.[e]	NB incor.[f] [%]
$(CF_3)FI$-Ni[a]	0.979	68	2.9	21	150	< 0.5
$(CF_3)FI^2$-Ni_2[b]	0.064	16	2.8	44	0.6	3.0
$(CH_3)FI$-Ni[a]	0.133	3.4	1.7	79	20	2.1
$(CH_3)FI^2$-Ni_2[b]	0.063	4.5	2.2	93	0.6	7.0

[a] Polymerizations carried out under constant 8.0 atm ethylene pressure with 5 μmol catalyst, 225 equiv of norbornene, and 2 equiv Ni(COD)$_2$/Ni for 10 min in 50 mL toluene. [b] Polymerizations carried out under constant 8.0 atm ethylene pressure with 10 μmol catalyst, 225 equiv of norbornene, and 2.0 equiv Ni(COD)$_2$/Ni for 40 min in 50 mL toluene. [c] From GPC versus polystyrene standards in (g mol^{-1}). [d] By ^1H NMR assay. [e] kg polymer mol^{-1}[Ni] h^{-1} atm^{-1}. [f] Molar percentage from ^{13}C NMR spectroscopy.[37]

more norbornene than does monometallic analogue **(CH$_3$)FI**-Ni (norbornene content = 7.0 vs. 2.1%, respectively). Fluoroalkyl-substituted catalysts **(CF$_3$)FI^2**-Ni$_2$ and **(CF$_3$)FI**-Ni introduce less norbornene than the methyl-substituted analogues, however, bimetallic **(CF$_3$)FI^2**-Ni$_2$ introduces six-times more norbornene than does its monometallic analogue **(CF$_3$)FI**-Ni (norbornene content = 3.0 vs. < 0.5%, respectively). In all cases, catalyst productivity is lower in the ethylene-*co*-norbornene polymerizations than in analogous ethylene homopolymerizations. The chain branch densities and PDI's of the ethylene-*co*-norbornene polymers are similar to those of the corresponding ethylene homopolymers.

Catalyst deactivation experiments: The catalyst deactivation products arising from ethylene polymerizations when using **(CH$_3$)FI^2-Ni$_2$** were investigated by analysis of the post-polymerization materials. Ethylene polymerizations were conducted under continuous 8.0 atm ethylene pressure at 50 °C for 50 min. After the desired run time, the reactor pressure was reduced to 1.0 atm ethylene pressure and the volatiles removed, in vacuo. ^{1}H NMR spectroscopic analysis of the residue indicates formation of the free ligand in addition to a large amount of black Ni^0. The free ligand formed during **(CF$_3$)FI^2**-Ni$_2$ deactivation can undergo further reaction with **(CF$_3$)FI^2**-Ni$_2$ and form 2 equiv **(CF$_3$)FI^2**-Ni**(OH)** (Scheme 8). Under the conditions investigated, no evidence of bis-ligated products is observed.[8,38]

Discussion

Ethylene homopolymerization: Several trends are evident when the ethylene polymerization characteristics of **(CH$_3$)FI^2**-Ni$_2$, **(CF$_3$)FI^2**-Ni$_2$, **(CH$_3$)FI**-Ni, and **(CF$_3$)FI**-Ni are compared. First, the installation of CF_3 substituents in **(CF$_3$)FI^2**-Ni$_2$ and **(CF$_3$)FI**-Ni produces polyethylenes with significantly higher molecular weight relative to the methyl-substituted terphenyl catalysts (M_w = 92 vs. 1.4 K, respectively, for **(CF$_3$)FI**-Ni and **(CH$_3$)FI**-Ni at room temperature). We have previously argued that weak C–F···H–C interactions between CF_3 substituents remote to the catalytic center and a C–H unit on the growing polymer chain likely disfavor chain transfer in **(CF$_3$)FI**-Ni by destabilizing the *syn*-periplanar conformation generally thought to facilitate β-H elimination (Scheme 3).[17] For catalyst **(CH$_3$)FI**-Ni, the absence of such interactions favors the correct conformation for elimination. We expect similar C–F···H–C interactions to be operative in **(CF$_3$)FI^2-Ni$_2$** and to be largely responsible for the dramatic differences in M_w and branching characteristics of the polyethylenes produced by **(CF$_3$)FI^2-Ni$_2$** versus **(CH$_3$)FI^2-Ni$_2$**. In terms of ethylene polymerization activity at 25 °C, mononuclear **(CF$_3$)FI-Ni** is 2.7-times more active than **(CH$_3$)FI-Ni**, whereas binuclear **(CF$_3$)FI^2-Ni$_2$** is 2.3-times more active than **(CH$_3$)FI^2-Ni$_2$**. At 25 °C, both mononuclear catalysts display higher ethylene polymerization activities than do the bimetallic analogues, presumably reflecting increased steric repulsion in the latter catalysts. At 50 °C, observed polymerization rates for CF_3-substituted terphenyl catalysts **(CF$_3$)FI^2**-Ni$_2$ and **(CF$_3$)FI**-Ni are increased relative to room temperature polymerizations, indicating enhanced thermal stability versus the CH_3– substituted analogues. The increased thermal stability of fluorinated catalysts **(CF$_3$)FI^2**-Ni$_2$ and **(CF$_3$)FI**-Ni may reflect suppression of β-H elimination via the aforementioned C–F···H–C interaction, since β-H elimination has been shown to be a key step in the deactivation of monometallic Ni^{II} ethylene polymerization catalysts,[38] and will also be shown to be important in the deactivation of the present bimetallic catalysts (vide infra). Non-fluorinated catalysts **(CH$_3$)FI^2**-Ni$_2$ and **(CH$_3$)FI**-Ni deactivate rapidly at 50 °C. The thermal stability of **(CH$_3$)FI^2**-Ni$_2$ and **(CF$_3$)FI^2**-Ni$_2$ was further investigated by conducting ethylene polymerizations at 50 °C for varying reaction times (Table 3, Figure 6). Although both bimetallic catalysts evidence a fall in ethylene activity over time, CF_3-substituted **(CF$_3$)FI^2**-Ni$_2$ displays significantly higher thermal stability than does **(CH$_3$)FI^2**-Ni$_2$. During ethylene polymerizations at 50 °C, all product polyethylene M_w values are depressed relative to 25 °C polymerizations, presumably reflecting more favorable/entropically driven β-H elimination at higher temperatures.

During attempts to identify the deactivation pathways that these catalysts might undergo at elevated temperatures, ethylene polymerizations were also conducted with **(CF$_3$)FI^2**-Ni$_2$ at 50 °C by using B(C_6F_5)$_3$ as the phosphine scavenging co-catalyst rather than Ni(COD)$_2$ (Table 2, entry 3). Interestingly, ethylene polymerizations utilizing B(C_6F_5)$_3$ as the co-catalyst are nearly 2.2-times more active than polymerizations for which Ni(COD)$_2$ is used as co-catalyst. This increased activity is likely due to more efficient phosphine abstraction by the very Lewis acidic B(C_6F_5)$_3$, forming the $Me_3P{\cdot}B(C_6F_5)_3$ adduct.[39] Additionally, the polyethylenes produced by **(CF$_3$)FI^2**-Ni$_2$ at 50 °C with B(C_6F_5)$_3$ as co-catalyst display monomodal GPC traces (Table 2, entry 3); analogous polymerizations with the use of Ni(COD)$_2$ lead to bimodal traces. In the absence of Ni(COD)$_2$ or B(C_6F_5)$_3$ co-catalysts, none of the present catalysts displays significant polymerization activity. Ni(COD)$_2$ and B(C_6F_5)$_3$ have been proposed to function as phosphine scavengers by abstracting PMe_3, thus opening a Ni coordination site for ethylene activation/-polymerization.[8d] In the present systems, two factors may be responsible for the co-catalyst requirement: 1) PMe_3 is significantly more basic[40] than PPh_3, which is typically used in catalyst systems that are active in the absence of phosphine scavenger, and 2) the prodigious steric encumbrance in these catalysts may impede associative ligand exchange between coordinated PMe_3 and incoming ethylene.[38b,41]

Catalyst cooperativity effects: Several groups have synthesized and investigated the ethylene polymerization characteristics of bimetallic neutrally charged Ni^{II} catalysts (Scheme 9).[1a,42] Where X-ray diffraction data are available, Ni···Ni distances are large, typically from 7.41 to 7.77 Å, and

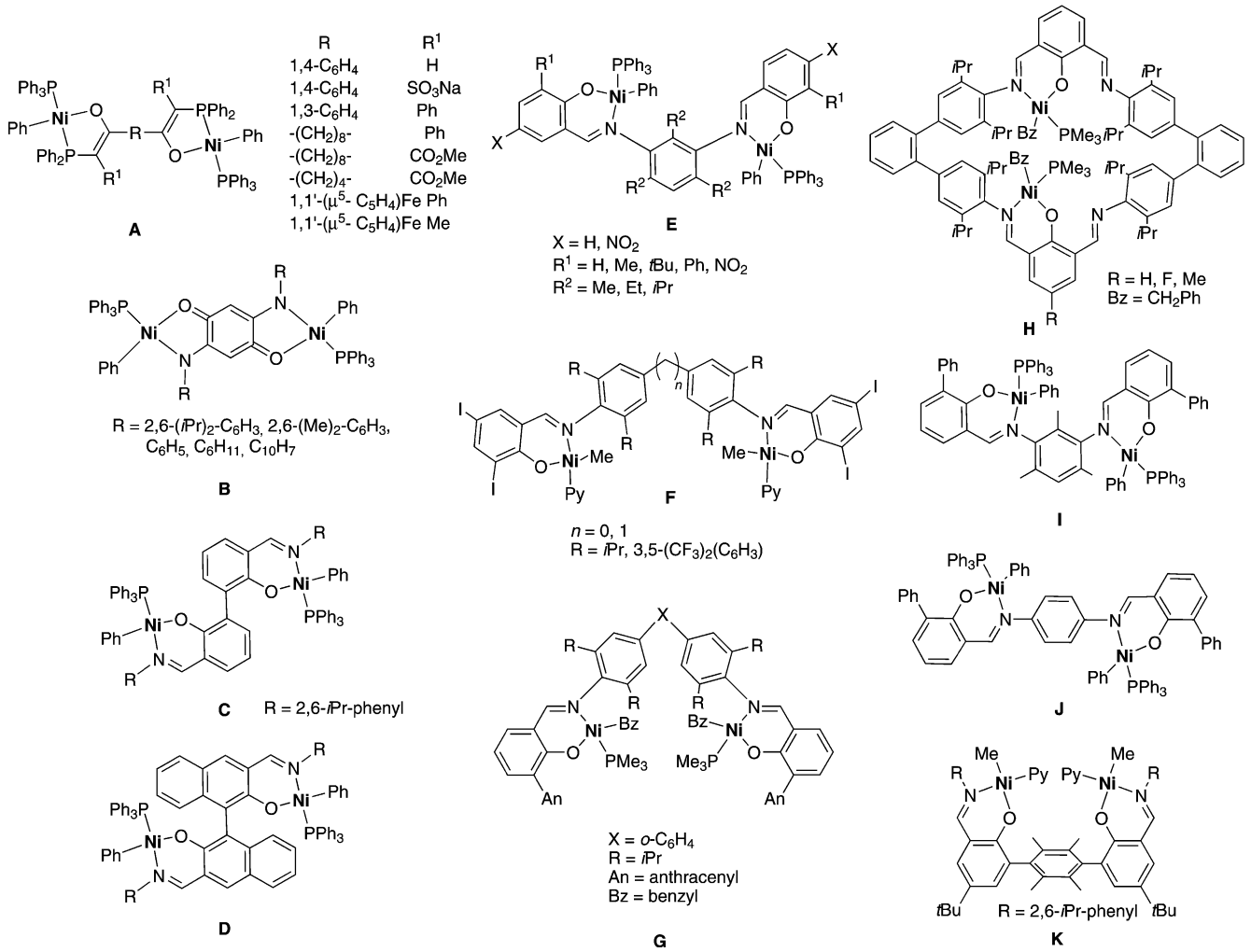

Scheme 9. Examples of previously reported bimetallic neutrally charged Ni^{II} polymerization catalysts (**A**–**J**,[1a] **K**[42]).

reported cooperative effects are minimal.[33a,b,d,42] In all of the present 25 °C ethylene polymerizations (Table 1), bimetallic catalysts **$(CH_3)FI^2$-Ni_2** and **$(CF_3)FI^2$-Ni_2** introduce significantly greater polyethylene branch densities than do the corresponding monometallic controls, presumably reflecting favorable agostic polymer C–H interactions between the growing polymer chain and the second proximate metal center, thus favoring branch formation (Scheme 10b).

By conducting ethylene polymerizations with **FI^2-Ni_2** over a range of ethylene pressures,[6] it was shown that the origin of the branching in these bimetallic catalysts is likely the same as in the monometallic analogues, that is, rapid "chain-walking" β-H elimination/reinsertion sequences.[38b] In the case of fluorocarbon-substituted catalysts **$(CF_3)FI^2$-Ni_2** and **$(CF_3)FI$-Ni**, polyethylene branching would also be affected by the proposed C–F···H–C interactions, which would suppress β-H elimination and chain-walking (Scheme 3). Thus, the marked increase in branch density in the polyethylenes produced by bimetallic **$(CF_3)FI^2$-Ni_2** relative to monometallic **$(CF_3)FI$-Ni** likely reflects the proximate metal centers and agostic C–H···Ni interactions that favor branch formation (e.g., Figure 1), which are expected to be stronger than the proposed C–F···H–C interactions.[43] At 50 °C, polyethylene branch densities are increased for all catalysts (Table 2) relative to 25 °C. In accord with this model, bimetallic **$(CF_3)FI^2$-Ni_2** displays significantly more branching than monometallic **$(CF_3)FI$-Ni**. At 50 °C, differences in branch densities introduced by catalysts **$(CH_3)FI^2$-Ni_2** and **$(CH_3)FI$-Ni** are similar.

In ethylene-*co*-norbornene polymerization experiments catalyzed by **$(CH_3)FI^2$-Ni_2** and **$(CF_3)FI^2$-Ni_2**, both catalysts display approximately 3–6-times greater selectivity for norbornene enchainment than do their monometallic counterparts (Table 4). These results parallel our previously reported bimetallic Ni^{II} catalyst, **FI^2-Ni_2** (Scheme 2), which displays somewhat greater (~3×) norbornene selectivity than its monometallic analogue.[20] Lee and co-workers also reported bimetallic Ni^{II} salicylaldimine catalysts that mediate ethylene + polar norbornene copolymerization (Scheme 9, **G**);[33c] although X-ray structural characterization of these catalysts was not reported, computational geometry optimizations suggest Ni···Ni distances ranging from 6.24–9.40 Å;

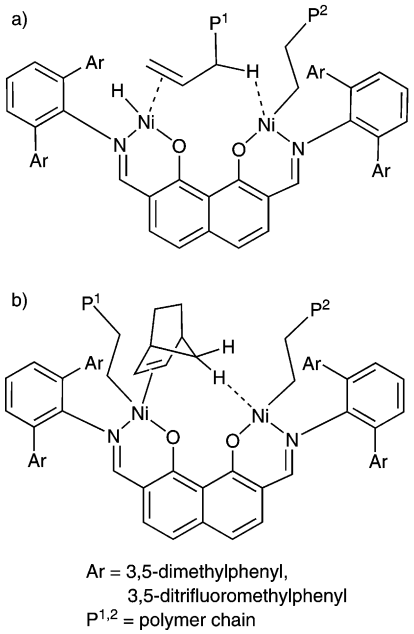

Scheme 10. a) Proposed secondary agostic interactions in bimetallic catalysts that may influence β-H elimination/re-insertion kinetics and afford increased chain branching. b) Proposed chelating π/agostic C–H intermediate facilitating increased norbornene incorporation in ethylene-*co*-norbornene polymerizations mediated by catalysts **$(CH_3)FI^2$-Ni_2** and **$(CF_3)FI^2$-Ni_2**.

these catalysts were reported to incorporate 2–3-times more polar-norbornene than a monometallic control. The greater selectivity for norbornene enchainment relative to the mononuclear catalysts reported here is consistent with the shorter Ni···Ni distance, which—all other factors being equal—would be expected to enhance catalyst center···catalyst center cooperativity (Scheme 9).

An attractive enchainment pathway is one in which norbornene π bonds to one Ni center and simultaneously binds to the second Ni center via an agostic interaction (Scheme 10b), thereby pre-organizing the monomer for enchainment (similar to the DFT-computed catalyst–octane interaction of Figure 1). Note that the present results reveal a significant decrease in copolymerization activity upon addition of the norbornene co-monomer. The reduced rate of ethylene-*co*-norbornene polymerizations versus corresponding ethylene polymerizations was observed previously in neutrally charged Ni^{II} catalysts.[14r] It is attributable to sluggish ethylene insertion into the severely encumbered Ni–norbornyl bond. Indeed, norbornene displays this type of chelating π donation/agostic bonding in several Rh, Ru, and Cu complexes (Scheme 11, **A**, **B**, and **C**, respectively).[44] Also, in norbornene homopolymerizations mediated by monometallic cationic (allyl)Pd catalysts, such γ-agostic species were recently shown to be a key intermediate (Scheme 11, **D**), and were fully characterized by X ray diffraction and NMR spectroscopy.[45]

Catalyst deactivation: At 50 °C, all the catalysts reported here, with the exception of **(CF_3)FI-Ni**, undergo decomposition to form black Ni^0. The deactivation pathway for monometallic neutrally charged nickel(II) phenoxyiminato catalysts is thought to involve reductive elimination of alkane through bimolecular [N,O]Ni–H + [N,O]Ni–alkyl reductive elimination (Scheme 12).[38a]

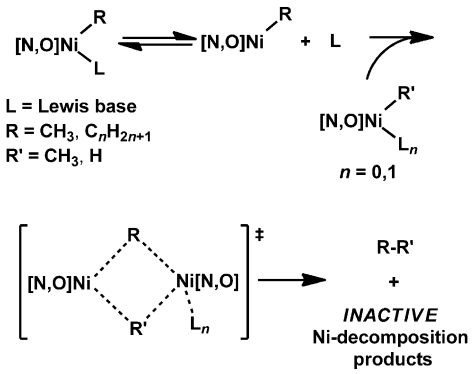

Scheme 12. Proposed deactivation pathway for monometallic phenoxyiminato Ni catalysts.

For monometallic catalysts **(CH_3)FI-Ni** and **(CF_3)FI-Ni**, our observations agree with this proposed pathway (Scheme 12). For bimetallic catalysts **$(CH_3)FI^2$-Ni_2** and **$(CF_3)FI^2$-Ni_2**-mediated ethylene polymerizations at 50 °C, Ni^0 is observed visually, and free ligand formation by in situ ^{1}H NMR spectroscopy. A pathway consistent with Ni^0, free

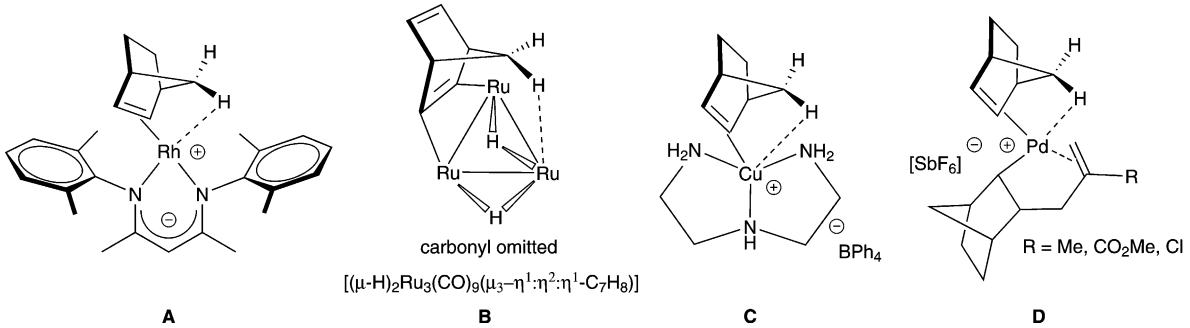

Scheme 11. Examples of Rh, Ru, Cu, and Pd norbornene complexes exhibiting γ-agostic interactions.

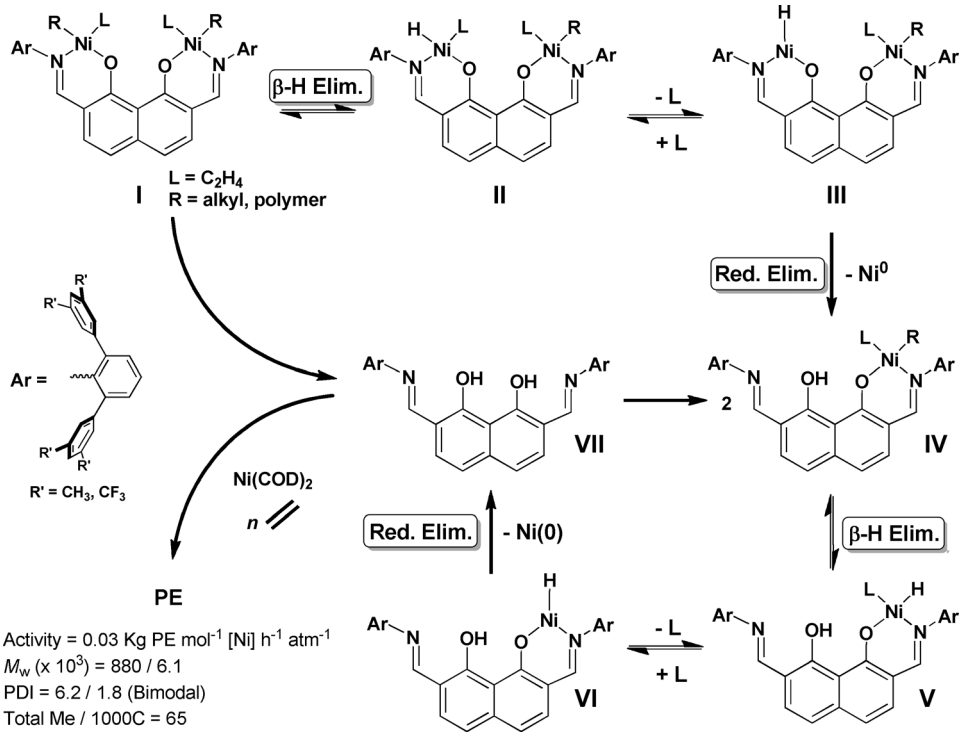

Scheme 13. Proposed thermal deactivation pathway for bimetallic catalysts **$(CH_3)FI^2$-Ni_2** and **$(CF_3)FI^2$-Ni_2**.

ligand, and our conclusion that the predominant chain transfer pathway in these catalysts is β-H elimination[17] (yielding Ni–H), is shown in Scheme 13. Here, elimination of a growing polymer chain via β-H transfer yields a Ni–H at one coordination site (**II**), which undergoes reductive elimination forming Ni^0 and one ligand O–H group (**IV**). Repetition then eliminates another Ni^0 moiety and free ligand (**VII**). Investigation of the reaction between **$(CF_3)H_2FI^2$** and **$(CF_3)FI^2$-Ni_2** (Scheme 8) confirms that liberated free ligand **VII** indeed undergoes reaction with the dinickel complex, forming 2 equiv monometallic Ni species **IV** (Scheme 13). A roughly analogous deactivation pathway was proposed for monometallic neutral Ni^{II} anilinotroponate ethylene polymerization catalysts in which an Ni–H group undergoes reductive elimination yielding Ni^0 and free ligand.[38b] At 50 °C, bimetallic catalysts **$(CH_3)FI^2$-Ni_2** and **$(CF_3)FI^2$-Ni_2** both produce polyethylene, which has a bimodal molecular weight distribution by GPC. For both catalysts, the minor component of the GPC trace is higher M_w polyethylene. As the polymerization time at 50 °C is increased, the proportion of the higher M_w polyethylene fraction increases (Figure 7). This observation suggests the formation of a new catalytic species during the deactivation of **$(CH_3)FI^2$-Ni_2** and **$(CF_3)FI^2$-Ni_2**. In room temperature ethylene polymerizations when using bimetallic **$(CH_3)FI^2$-Ni_2** and **$(CF_3)FI^2$-Ni_2**, the product polymers display monomodal GPC traces if the polymerization time is held to 40 min. However, when the polymerization time is increased to 120 min, a high M_w shoulder, reminiscent of the high M_w polymer formed at 50 °C, appears.[46] To determine if species **IV** might be responsible for the high M_w fraction, the ethylene polymerization properties of **$(CF_3)FI^2$-Ni(OH)** were investigated. Complex **$(CF_3)FI^2$-Ni(OH)**, when activated with $Ni(COD)_2$, is an active ethylene polymerization catalyst at room temperature and at 50 °C (Tables 2 and 3). At 25 °C, **$(CF_3)FI^2$-Ni(OH)** exhibits four-times the activity of bimetallic **$(CF_3)FI^2$-Ni_2**, and at 50 °C, 20.7 greater activity than bimetallic **$(CF_3)FI^2$-Ni_2** under the same polymerization conditions. Microstructural analysis of the polyethylenes produced by **$(CF_3)FI^2$-Ni(OH)** indicates lower M_w polyethylene with similar branch numbers versus the polyethylenes produced by **$(CF_3)FI^2$-Ni_2**. In previous work, the effects of installing an intramolecular hydrogen bond directed toward

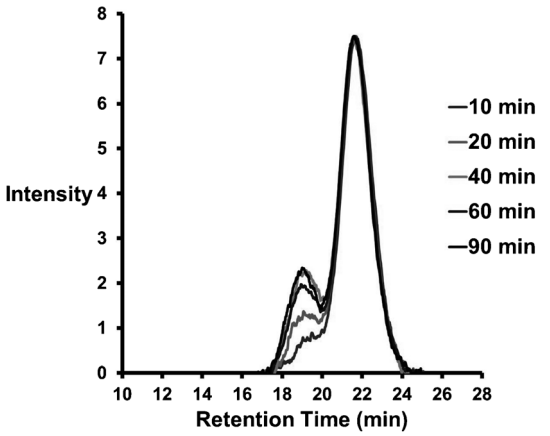

Figure 7. Normalized GPC traces with viscometry detection of polyethylenes derived from catalyst **$(CF_3)FI^2$-Ni_2** at 50 °C under 8.0 atm ethylene pressure, showing the appearance of a higher M_w polyethylene fraction as polymerization time is increased.

a polymerization-active Ni^{II} center were investigated,[14c] and it was concluded that installing the hydrogen bond adjacent to the Ni center leads to a more electron-deficient catalyst as shown below; see also ref. [14c]), increasing ethylene polymerization activity and depressing product polyethylene M_w. Similar conclusions can be drawn here when the polymerization results for **$(CF_3)FI^2$-Ni(OH)** and **$(CF_3)FI^2$-Ni_2** are compared. GPC analysis of the polyethylenes obtained at 50 °C from **$(CF_3)FI^2$-Ni(OH)** shows that this complex is not responsible for the high M_w shoulder present in the GPC

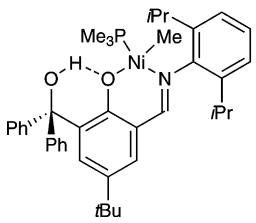

trace of the polyethylenes produced by **$(CF_3)FI^2$-Nii_2** at 50 °C. However, the data (Figure 8) suggest that the polyethylene produced by **$(CF_3)FI^2$-Ni(OH)** is very similar to the major polyethylene peak produced by

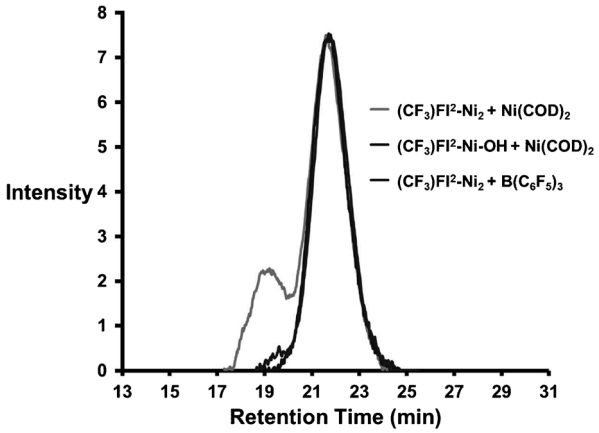

Figure 8. Normalized GPC with viscometer detection of polyethylenes derived from catalyst **$(CF_3)FI^2$-Ni(OH)** (Table 2, entry 5, 0.5 μmol) activated with $Ni(COD)_2$, and **$(CF_3)FI^2$-Ni$_2$** activated with $Ni(COD)_2$ or $B(C_6F_5)_3$ at 50 °C under constant 8.0 atm ethylene pressure.

$(CF_3)FI^2$-Ni$_2$ at 50 °C, arguing that intermediate **IV** (Scheme 13) is responsible for significant polyethylene production when bimetallic catalysts **$(CH_3)FI^2$-Ni$_2$** and **$(CF_3)FI^2$-Ni$_2$** are employed at 50 °C. Due to the high polymerization activity of **$(CF_3)FI^2$-Ni(OH)** relative to **$(CF_3)FI^2$-Ni$_2$**, a small amount of **$(CF_3)FI^2$-Ni(OH)** produced during **$(CF_3)FI^2$-Ni$_2$** deactivation is capable of producing the bulk of the polymeric product. Note that polyethylenes produced at 50 °C when using **$(CF_3)FI^2$-Ni(OH)** as catalyst are monomodal when the catalyst loading is low (0.5 μmol; Figure 8). However, the deactivation pathway depicted in Scheme 13 suggests that **$(CF_3)FI^2$-Ni(OH)** should produce bimodal polyethylene similar to **$(CF_3)FI^2$-Ni$_2$**. However, it is likely that, due to the low catalyst concentration used in these polymerizations, the amount of polyethylene produced by reaction of free ligand, arising from deactivation of **$(CF_3)FI^2$-Ni(OH)**, and $Ni(COD)_2$ is a very minor component. Furthermore, when polymerizations are conducted at higher catalyst loadings (5.0 μmol) a bimodal polyethylene is obtained (Figure S22 in the Supporting Information) with a high M_w shoulder similar to the GPC traces of the polyethylenes produced at 50 °C by **$(CF_3)FI^2$-Ni$_2$** (Figure 7).

To help identify the species producing the high M_w polymer in polymerizations with **$(CH_3)FI^2$-Ni$_2$** and **$(CF_3)FI^2$-Ni$_2$** at 50 °C, ethylene polymerizations were performed by using **$(CF_3)FI^2$-Ni$_2$** with $B(C_6F_5)_3$ as the co-catalyst at 50 °C (Table 2). In addition to approximately 2.2-times increase in activity, GPC analysis of the polyethylenes obtained with **$(CF_3)FI^2$-Ni$_2$** + $B(C_6F_5)_3$ showed the absence of the high M_w fraction that was observed in analogous polymerizations when using $Ni(COD)_2$ as co-catalyst (Figure 8). From these observations, it appears likely that $Ni(COD)_2$ contributes to the formation of the high M_w polymer in the polyethylenes produced by **$(CH_3)FI^2$-Ni$_2$** and **$(CF_3)FI^2$-Ni$_2$** at 50 °C. Keim and Peuckert[47] showed that $Ni(COD)_2$ undergoes reaction with $Ph_2PCH_2CO_2H$, to yield the active ethylene oligomerization catalyst [P,O]Ni(η^3-C_8H_{13}). Indeed, in the presence of other bidentate ligands with acidic hydrogen atoms, such as hexafluoroacetylacetone, $Ni(COD)_2$ is also active for ethylene oligomerization.[48] Based on deuterium labeling experiments, it was shown that the formation of the active catalyst occurs by direct protonation of an electron-rich Ni-coordinated alkene. $Ni(COD)_2$ was also shown to be an active ethylene polymerization catalyst in the presence of $[H(Et_2O)_2]^+[B(C_6F_5)_4]^-$ (an acid source) with amidodiphosphine ligand $\{(Ar)_2P\}_2NMe$ (PNP).[49] Furthermore, Jordan and co-workers concluded that the polymerization-active species is $[(PNP)Ni(CODH)]^+[B(C_6F_5)_4]^-$, generated by protonation of (PNP)Ni(COD) with $[H(Et_2O)_2]^+[B(C_6F_5)_4]^-$ (Scheme 14).[49a]

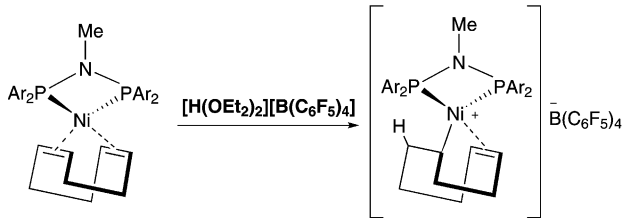

Scheme 14. Formation of an active ethylene polymerization catalyst from an $L_2Ni(COD)$ complex.

In the pathway shown in Scheme 13, free ligand and Ni^0 are produced during the deactivation of **$(CH_3)FI^2$-Ni$_2$** and **$(CF_3)FI^2$-Ni$_2$** activated by $Ni(COD)_2$. The results above show that $Ni(COD)_2$ in the presence of a protic ligand can afford active ethylene oligomerization/polymerization-active species. Since $Ni(COD)_2$ is used in excess in the polymerizations reported here, free $Ni(COD)_2$ is doubtless present. To investigate any additional role $Ni(COD)_2$ might play (other than phosphine abstraction) in these polymerizations, reactions were also conducted at 50 °C by using a combination of the free **$(CF_3)H_2FI^2$** ligand and $Ni(COD)_2$ (Table 2). In situ reaction of **$(CF_3)H_2FI^2$** and $Ni(COD)_2$ results in the production of polyethylene with low activity (0.03 kg polyethylene $mol^{-1}[Ni]\,h^{-1}\,atm^{-1}$), and GPC analysis of the polyethylenes produced by **$(CF_3)H_2FI^2$**/$Ni(COD)_2$ reveals a bimodal behavior with one very high M_w component (880 K) with a large PDI (6.1), and one component with a M_w more typical of the systems investigated here (6.1 K). These results argue that $Ni(COD)_2$ is a "non-innocent" co-catalyst (phosphine-scavenger), and that reaction of $Ni(COD)_2$ with free ligand, generated during **$(CH_3)FI^2$-Ni$_2$** and **$(CF_3)FI^2$-Ni$_2$** catalyst thermolysis at 50 °C, plausibly yields a catalytic species accounting for the high M_w fraction in the product GPCs from the bimetallic catalysts.[50] Further support for this hypothesis comes from the observation that the use of

$B(C_6F_5)_3$ as a co-catalyst in place of $Ni(COD)_2$ suppresses the production of the high molecular weight fraction.

Conclusion

Two new sterically encumbered Ni^{II} bimetallic ethylene polymerization catalysts, **$(CH_3)FI^2$-Ni_2** and **$(CF_3)FI^2$-Ni_2**, were synthesized and fully characterized. These catalysts are active ethylene polymerization catalysts in the presence of the phosphine scavengers/co-catalysts $Ni(COD)_2$ or $B(C_6F_5)_3$. Catalyst center···catalyst center cooperative effects are observed in ethylene-*co*-norbornene polymerizations, with bimetallic catalysts **$(CH_3)FI^2$-Ni_2** and **$(CF_3)FI^2$-Ni_2** enchaining three- and six-times, respectively, more norbornene than their monometallic analogues **$(CH_3)FI$-Ni** and **$(CF_3)FI$-Ni**. The catalytic performance of **$(CH_3)FI^2$-Ni_2** and **$(CF_3)FI^2$-Ni_2** exhibits greater thermal stability than previous, less encumbered Ni_2 catalysts, and at 50 °C, all of the new catalysts exhibit appreciable ethylene polymerization activity. However, **$(CH_3)FI$-Ni**, **$(CH_3)FI^2$-Ni_2**, and **$(CF_3)FI^2$-Ni_2** evidence gradual deactivation at 50 °C. The deactivation pathway for **$(CH_3)FI^2$-Ni_2** and **$(CF_3)FI^2$-Ni_2** was investigated, and key steps are proposed to be the reductive elimination from Ni–H groups to form free (protonated) ligand and Ni^0. An ethylene polymerization-active intermediate **$(CF_3)FI^2$-Ni(OH)** (**IV** in Scheme 13) in the deactivation process is identified as that responsible for significant polyethylene production when the bimetallic catalysts are utilized at 50 °C. The free ligand formed in situ during bimetallic catalyst deactivation can then undergo reaction with a dinickel species (**I** in Scheme 13) to yield 2 equiv polymerization-active intermediate **$(CF_3)FI^2$-Ni(OH)**. Additionally, the free ligand can react with the $Ni(COD)_2$ co-catalyst, yielding a species capable of producing very high M_w polyethylene, which is very unusual for group 10 catalysts. In place of $Ni(COD)_2$, ethylene polymerizations co-catalyzed by $B(C_6F_5)_3$ led to monomodal polyethylene production at higher activities.

Experimental Section

Materials and methods: All manipulations of air-sensitive materials were performed with rigorous exclusion of O_2 and moisture in oven-dried Schlenk-type glassware on a dual manifold Schlenk line, interfaced to a high-vacuum line (10^{-6} Torr), or in a N_2-filled vacuum atmospheres glove box with a high capacity recirculator (<1 ppm O_2). Argon (Airgas, prepurified grade) was purified by passage through a supported MnO oxygen-removal column and an activated Davison 4A molecular sieve column. Ethylene (Airgas) was purified by passage through an O_2/moisture trap (Matheson, model MTRP-0042-XX). Norbornene was dried over sodium and transferred, in vacuo, to a Teflon-sealed storage flask. Diethyl ether and tetrahydrofuran were distilled from Na/benzophenone ketyl. Hydrocarbon solvents (benzene, *n*-pentane, *n*-hexane, toluene) were vacuum transferred from Na/K alloy. [D_6]Benzene (Cambridge Isotope Laboratories, 99+atom%D) was stored over Na/K alloy, in vacuo, and vacuum transferred immediately prior to use. All other deuterated solvents were used as received (Cambridge Isotope Laboratories, 99+atom%D). Tris(pentafluorophenyl)borane, $B(C_6F_5)_3$, was a gift from Albemarle Corporation (Baton Rouge, LA). The borane was purified by high-vacuum sublimation (80 °C/10^{-6} Torr). The reagents *trans*-NiMeCl-$(PMe_3)_2$,[29] 2,7-diformyl-1,8-dihydroxynaphthalene (**1**),[10a,21] and the terphenyl amines[22] were prepared according to literature procedures. $Ni(COD)_2$ (COD = 1,5-cyclooctadiene) was purchased from Strem; *p*-toluenesulfonic acid monohydrate and formic acid were purchased from Sigma–Aldrich. The monometallic catalysts **$(CH_3)FI$-Ni** and **$(CF_3)FI$-Ni** were prepared according to literature procedures.[17]

Physical and analytical measurements: NMR spectra were taken on Varian Hg400 (400 MHz, ^1H; 100 MHz, ^{13}C; 162 MHz, ^{31}P; 376 MHz, ^{19}F), Varian Ic 400 (400 MHz, ^1H; 100 MHz, ^{13}C), Varian Inova 500 (500 MHz, ^1H), and a Bruker Avance III 500 (500 MHz, ^1H; 125 MHz, ^{13}C) NMR spectrometers. Chemical shifts (δ) for ^1H and ^{13}C are referenced to TMS, internal solvent resonances relative to TMS, and the polymer CH_2 backbone. Chemical shifts (δ) for ^{31}P and ^{19}F are referenced to the external standards 85% H_3PO_4 and $CFCl_3$ dissolved in $CDCl_3$, respectively. NMR spectra of air-sensitive samples were acquired in Teflon valve sealed J. Young NMR tubes. NMR analysis of polymers was carried out in 1,1,2,2-[D_2]tetrachloroethane at 120 °C with d1 = 10 s. Polymer NMR spectra were assigned, and polyethylene branch numbers were calculated, according to the literature procedures for polyethylene[33a,d,e,35] and ethylene-*co*-norbornene.[37] Gel permeation chromatography (GPC) was carried out in 1,2,4-trichlorobenzene (stabilized with 125 ppm BHT) at 150 °C on a Polymer Laboratories 220 instrument equipped with a set of three PLgel 10 μm mixed-B LS columns with differential refractive index and viscosity detectors. Molecular weights were determined through universal calibration relative to polystyrene standards. Elemental analyses were performed by Midwest Microlabs, Indianapolis, Indiana.

Synthesis of 2,7-di[2,6-(3,5-dimethylphenyl)]imino-1,8-dihydroxynaphthalene, $(CH_3)H_2FI_2$: Under N_2, a Schlenk flask (100 mL) was charged with activated molecular sieves (1.7 g), 0.241 g (1.12 mmol) of 2,7-diformyl-1,8-dihydroxynaphthalene (**1**), 1.35 g (4.48 mmol) of 2,6-(3,5-dimethylphenyl)aniline, benzene (35 mL), and formic acid (5 drops). The resulting mixture was refluxed for 7 days during which time the reaction color changed from orange to red. The reaction mixture was allowed to cool and was then filtered to remove the sieves. The volatiles were next removed from the filtrate, in vacuo, and the resulting dark red oil was triturated with methanol, affording an orange solid. The orange solid was washed with diethylether, cooled to −10 °C, and filtered. This red solid was recrystallized from a 1:9.5 mixture of toluene and methanol, affording 0.357 g (0.456 mmol, 41% yield) of microcrystalline red solid. ^1H NMR (500 MHz, $CDCl_3$, 25 °C, TMS): δ = 14.14 (s, O*H*), 13.47 (d, N*H*), 8.50 (s, *H*C=N), 7.87 (d, NH-C*H*=C), 7.37 (s, Ar), 7.23–7.11 (m, Ar), 7.08 (s, Ar), 7.05 (s, Ar), 7.02 (s, Ar), 6.82 (s, Ar), 6.77 (s, Ar), 6.42 (d, Ar), 6.22 (d, Ar), 2.33 (s, H_3C-Ar), 2.24 ppm (s, H_3C-Ar); ^{13}C NMR (125 MHz, $CDCl_3$, 25 °C, TMS): δ = 183.98, 163.68, 159.83, 158.12, 149.78, 141.38, 140.00, 138.78, 137.81, 136.96, 135.96, 133.62, 130.66, 129.57, 129.47, 128.25, 127.90, 127.01, 126.81, 123.68, 118.67, 116.72, 116.30, 115.65, 108.60, 21.31 ppm; elemental analysis calcd (%) for $C_{56}H_{50}N_2O_2$: C 85.90, H 6.44, N 3.58; found: C 86.04, H 6.59, N 3.71.

Synthesis of 2,7-di[2,6-(3,5-di-trifluormethylphenyl)]imino-1,8-dihydroxynaphthalene, $(CF_3)H_2FI^2$: A round-bottom flask (250 mL) was charged with 0.709 g (3.28 mmol) of 2,7-diformyl-1,8-dihydroxynaphthalene (**1**), 3.90 g (7.54 mmol) of 2,6-(3,5-di-trifluoromethylphenyl)aniline, 62 mg (0.33 mmol) of *p*-toluenesulfonic acid monohydrate, and toluene (70 mL). The reaction mixture was refluxed by using a Dean–Stark trap for 3 days. The solvent was then removed under reduced pressure, and the resulting orange oil was triturated with methanol affording a red solid. This solid was washed with methanol (20 mL) to remove the half-condensation product. The excess aniline was then removed by recrystallizing the solid from a 1:9.5 mixture of toluene and methanol. This afforded 3.04 g (2.50 mmol, 76% yield) of red solid. Crystals suitable for X-ray analysis were obtained by slow evaporation of a $CDCl_3$ solution of **$(CF_3)H_2FI^2$**. ^1H NMR (500 MHz, $CDCl_3$, 25 °C, TMS): δ = 13.62 (d, N*H*), 13.32 (s, O*H*), 8.39 (s, *H*C=N), 7.92 (s, Ar), 7.74 (s, Ar), 7.57 (s, Ar), 7.51 (d, Ar), 7.40 (m, Ar), 7.02 (d, Ar), 6.83 (d, Ar), 6.50 (d, Ar), 6.24 ppm (d, Ar); ^{13}C NMR (125 MHz, $CDCl_3$, 25 °C, TMS): δ = 184.77, 163.91, 161.71, 157.36, 150.02, 142.44, 141.76, 139.62, 134.82, 134.11, 132.92, 132.65, 132.21, 131.52, 131.29, 130.98, 130.84, 130.54, 129.67, 129.19, 128.77,

128.38, 128.33, 125.44, 125.29, 124.58, 124.11, 122.40, 122.29, 121.93, 120.59, 118.15, 117.85, 115.94, 109.62, 21.56 ppm; ^{19}F NMR (376 MHz, $CDCl_3$, 25 °C): $\delta = -63.41$, -63.56 ppm; elemental analysis calcd (%) for $C_{56}H_{26}N_2F_{24}O_2$: C 55.73, H 2.16, N 2.31; found: C 55.02, H 2.31, N 2.27.

Representative procedure for the synthesis of sodium salts $(CH_3)FI^2$-Na_2 and $(CF_3)FI^2$-Na_2: Under N_2, a Schlenk flask (100 mL) was charged with 2.66 g (2.19 mmol) of **$(CF_3)H_2FI^2$** and 0.210 g (8.75 mmol) of NaH. To this was added dry THF (30 mL) via syringe. This red-orange mixture was allowed to stir for 48 h. The reaction mixture was then filtered and the volatiles were removed, in vacuo. The resulting red-orange solid was washed with *n*-pentane (50 mL) and dried under high vacuum, overnight, yielding 2.42 g (1.93 mmol, 88 % yield) of orange solid.

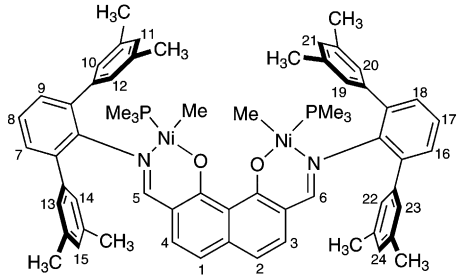

$(CH_3)FI^2$-Ni_2

Synthesis of {2,7-di-[2,6-(3,5-di-methylphenylimino)methyl]-1,8-naphthalenediolato}-bis-Ni^{II}-(methyl)(trimethylphosphine), $(CH_3)FI^2$-Ni_2: Dry benzene (20 mL) was added to a flask containing 0.590 g (0.713 mmol) of **$(CH_3)FI^2$-Na_2**. This mixture was then added slowly via cannula to a benzene solution (30 mL) of 0.373 g (1.43 mmol) of *trans*-NiMeCl$(PMe_3)_2$. An immediate red color change was observed. Due to the low solubility of **$(CH_3)FI^2$-Na_2** in benzene, the reaction mixture was transferred via cannula back to the original **$(CH_3)FI^2$-Na_2** flask. The reaction mixture was allowed to stir at room temperature, overnight. The reaction mixture was then filtered and the filtrate was concentrated, in vacuo. Dry *n*-pentane (15 mL) was then added via syringe, precipitating an orange solid. After filtration and drying under high vacuum, 0.654 g (0.605 mmol, 85 %) of **$(CH_3)FI^2$-Ni_2** was isolated. ^{1}H NMR (500 MHz, [D_6]benzene, 25 °C, TMS): $\delta = 7.74$ (d, $^4J_{PH} = 8.6$ Hz, 2H, 5- and 6-H), 7.58 (s, 4H, 10-, 12-, 13-, 14-H), 7.44 (d, $^3J(H,H) = 7.7$ Hz, 2H, 7- and 9-H), 7.36 (d, $^3J(H,H) = 7.5$ Hz, 2H, 16- and 18-H), 7.19, −7.12 (m, 6H, 8-, 17-, 19-, 20-, 22-, 23-H), 6.82 (s, 2H, 11- and 15-H), 6.75 (s, 2H, 21- and 24-H), 6.66 (d, $^3J(H,H) = 8.4$ Hz, 2H, 3- and 4-H), 6.36 (d, $^3J(H,H) = 8.4$ Hz, 2H, 1- and 2-H), 2.23 (s, 12H, Ar-CH_3), 2.12 (s, 12H, Ar-CH_3), 0.97 (d, $^2J(P,H) = 9.2$ Hz, 18H, P(CH_3)$_3$), −0.97 ppm (d, $^3J(P,H) = 7.1$ Hz, 6H, Ni-CH_3); ^{13}C NMR (125 MHz, [D_6]benzene, 25 °C, TMS): $\delta = 169.65$, 166.07, 150.16, 144.82, 141.19, 141.19, 141.03, 137.61, 137.30, 137.27, 136.90, 133.80, 130.53, 130.32, 128.91, 128.85, 128.59, 128.35, 128.16, 127.97, 125.28, 124.08, 115.24, 113.49, 21.65, 13.89 (d, $^1J(P,C) = 26.3$ Hz, P(CH_3)$_3$, −13.44 ppm (d, $^2J(P,C) = 43.6$ Hz, Ni-CH_3); ^{31}P NMR (162 MHz, [D_6]benzene, 25 °C): $\delta = -10.42$ ppm; elemental analysis calcd (%) for $C_{64}H_{72}N_2Ni_2O_2P_2$: C 71.13, H 6.72, N 2.59; found: C 71.25, H 6.67, N, 2.60.

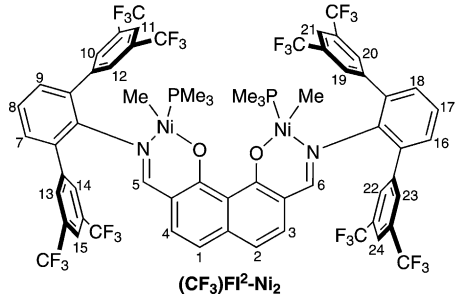

$(CF_3)FI^2$-Ni_2

Synthesis of {2,7-di-[2,6-(3,5-di-trifluoromethylphenylimino)methyl]-1,8-naphthalenediolato}-bis-Ni^{II}-(methyl)(trimethylphosphine), $(CF_3)FI^2$-Ni_2: A Schlenk flask (100 mL) was charged with 2.00 g (1.50 mmol) of **$(CF_3)FI^2$-Na_2** and 0.785 g (3.00 mmol) of *trans*-NiMeCl$(PMe_3)_2$. Toluene (150 mL) was added to this mixture via cannula at −78 °C. The reaction mixture was allowed to stir at −78 °C for 15 min. The reaction mixture was then warmed to −42 °C and stirred for 3.5 h after which time the reaction mixture turned red. The reaction mixture was then placed in a −10 °C water bath and stirred for 75 min. The resulting cerise-colored reaction mixture was then allowed to warm to room temperature and was stirred for an additional 3 h. The reaction mixture was then filtered and the volatiles were removed from the filtrate, in vacuo. The solid obtained next was triturated with *n*-pentane to yield 1.60 g (1.06 mmol, 73 % yield) of red solid. Single crystals suitable for X-ray diffraction were grown from the slow evaporation of an *n*-hexane solution in the glovebox. ^{1}H NMR (500 MHz, [D_6]benzene, 25 °C, TMS): $\delta = 8.29$ (s, 4H, 10-, 12-, 13-, and 14-H), 7.73 (s, 2H, 11- and 15-H), 7.68 (s, 2H, 21- and 24-H), 7.63 (s, 4H, 19-, 20-, 22-, and 23-H), 6.97–6.90 (m, 6H, 5-, 6-, 7-, 8-, 9-, and 17-H), 6.80 (dd, $^3J(H,H) = 6.9$ Hz, $^4J(H,H) = 2.3$ Hz, 2H, 16-, and 18-H), 6.38 (d, $^3J(H,H) = 8.4$ Hz, 2H, 3- and 4-H), 6.26 (d, $^3J(H,H) = 8.4$ Hz, 2H, 1- and 2-H), 0.81 (d, $^2J(P,H) = 9.9$ Hz, 9H, P(CH_3)$_3$), −1.36 ppm (d, $^3J(P,H) = 6.5$ Hz, 6H, Ni-CH_3); ^{13}C NMR (125 MHz, [D_6]benzene, 25 °C, TMS): $\delta = 170.15$, 165.53, 150.16, 145.78, 142.76, 142.12, 134.45, 134.20, 133.79, 131.78, 131.51, 131.27, 130.88, 130.77, 125.87, 125.07, 124.97, 123.49, 122.90, 122.80, 120.94, 114.94, 13.28 (d, $^1J(P,C) = 28.5$ Hz, P(CH_3)$_3$), −13.61 ppm (d, $^2J(P,C) = 44.6$ Hz, Ni-CH_3); ^{31}P NMR (162 MHz, [D_6]benzene, 25 °C): $\delta = -9.46$ ppm; ^{19}F NMR (376 MHz, [D_6]benzene, 25 °C): $\delta = -62.89$, -63.07 ppm; elemental analysis calcd (%) for $C_{64}H_{48}N_2F_{24}Ni_2O_2P_2$: C 50.83, H 3.20, N 1.85; found: C 50.98, H 3.39, N 1.85.

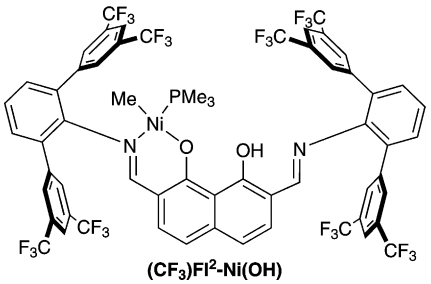

$(CF_3)FI^2$-Ni(OH)

Synthesis of {2,7-di-[2,6-(3,5-di-trifluoromethylphenylimino)methyl]-1-hydroxy-8-naphthalene-diolato}-Ni^{II}-(methyl)(trimethylphosphine), $(CF_3)FI^2$-Ni(OH): A Schlenk flask (25 mL) was charged with 0.240 g (0.198 mmol) of **$(CF_3)H_2FI^2$**, 0.300 g (0.198 mmol) of **$(CF_3)FI^2$-Ni_2**, and toluene (20 mL). The resulting red solution was then stirred at 50 °C, overnight, after which the volatiles were removed, in vacuo, leaving a red solid. The solid obtained was triturated with *n*-pentane and dried under vacuum affording 0.401 g (0.294 mmol, 74 % yield) of orange solid. ^{1}H NMR (500 MHz, [D_6]benzene, 25 °C, TMS): $\delta = 12.83$ (s, 1H, O*H*), 8.31 (s, 1H, Ar-*H*), 8.09 (d, 1H, Ar-*H*), 7.91 (s, 4H, Ar-*H*), 7.89 (s, 4H, Ar-*H*), 7.75 (s, 2H, Ar-*H*), 7.69 (s, 2H, Ar-*H*), 6.98–6.88 (m, 6H, Ar-*H*), 6.86 (s, 1H, Ar-*H*), 6.78 (d, 1H, Ar-*H*), 6.44 (d, 1H, Ar-*H*), 6.26 (d, 1H, Ar-*H*), 0.54 (s, 9H, P(CH_3)$_3$), −1.34 ppm (s, 3H, Ni-CH_3); ^{13}C NMR (125 MHz, [D_6]benzene, 25 °C, TMS): $\delta = 167.88$, 166.50, 162.56, 161.75, 150.53, 149.74, 142.44, 142.31, 141.62, 133.77, 132.26, 131.99, 131.86, 131.73, 131.60, 131.46, 131.33, 131.07, 130.97, 130.78, 130.74, 127.46, 127.30, 127.07, 126.71, 125.13, 125.08, 124.90, 122.96, 122.73, 121.25, 120.79, 120.50, 118.81, 116.86, 116.66, 115.93, 112.86, 12.37, −13.65 ppm; ^{31}P NMR (162 MHz, [D_6]benzene, 25 °C): $\delta = -12.06$ ppm; ^{19}F NMR (376 MHz, [D_6]benzene, 25 °C): $\delta = -63.11$, -63.23 ppm; elemental analysis calcd (%) for $C_{60}H_{37}N_2F_{24}NiO_2P$: C 52.85, H 2.73, N 2.05; found: C 52.62, H 2.78, N 2.13.

General procedure for ethylene polymerization experiments: In a typical experiment, an oven-dried thick-walled glass pressure vessel (350 mL)

was charged in the glovebox with Ni catalyst (5 μmol), 2.0 equiv Ni(COD)$_2$ per Ni, dry toluene (50 mL), and a large magnetic stir bar. The pressure vessel was then interfaced to a high-pressure line and the solution was degassed. The reactor was warmed to the desired temperature by using a water or oil bath, and allowed to equilibrate for 5 min. With rapid stirring, the reactor was then pressurized to 8.0 atm pressure ethylene, which was maintained during the course of the polymerization. After the desired run time, the reactor was vented and the contents poured into acidic methanol. The precipitated polymer was collected by filtration, washed with methanol, and dried at 60 °C, overnight, under high vacuum.

General procedure for ethylene polymerization experiments with catalyst (CF$_3$)FI^2-Ni(OH) (Table 2, entry 4): An oven-dried thick-walled glass pressure vessel (350 mL) was charged in the glovebox with 1 mL (0.5 μmol) of a 0.5 mM dry toluene solution of **(CF$_3$)FI^2-Ni(OH)**, 2.0 equiv Ni(COD)$_2$ per Ni, dry toluene (49 mL), and a large magnetic stir bar. The pressure vessel was then interfaced to a high-pressure line and the solution was degassed. The reactor was warmed to 50 °C by using an oil bath, and allowed to equilibrate for 5 min. With rapid stirring, the reactor was then pressurized to 8.0 atm pressure ethylene, which was maintained during the course of the polymerization. After the desired run time (40 min), the reactor was vented and the contents poured into acidic methanol. The precipitated polymer was collected by filtration, washed with methanol, and dried at 60 °C, overnight, under high vacuum.

General procedure for ethylene-*co*-norbornene polymerization experiments: In a typical experiment, an oven-dried thick-walled glass pressure vessel (350 mL) was charged in the glovebox with Ni catalyst (5.0 μmol), 2.0 equiv Ni(COD)$_2$ per Ni, dry toluene (23.5 mL), and a large magnetic stir bar. The pressure vessel was then interfaced to a high-pressure line and the solution was degassed. The reactor was warmed to the desired temperature by using a water or oil bath, and allowed to equilibrate for 5 min. The reactor was then pressurized to 1.0 atm ethylene pressure and 1.5 mL from a 0.74 M norbornene solution in toluene was immediately injected. The norbornene solution had been degassed and the aliquot was taken under an atmosphere of purified ethylene. With rapid stirring, the reactor was then pressurized to 8.0 atm ethylene pressure, which was maintained during the course of the polymerization. After the desired run time, the reactor was vented and the reaction mixture was poured into acidic methanol. The precipitated polymer was collected by filtration, washed with methanol, and dried at 60 °C, overnight, under high vacuum.

General procedure for analysis of ethylene polymerization deactivation products: An oven-dried thick walled glass pressure vessel (350 mL) was charged in the glovebox with 10.8 mg (10.0 μmol) **(CH$_3$)FI^2-Ni$_2$**, 11.0 mg (40.0 μmol) Ni(COD)$_2$, dry toluene (25 mL), and a large magnetic stir bar. The pressure vessel was then interfaced to a high-pressure line and the solution was degassed. The reactor was next warmed to 50 °C by using an oil bath, and allowed to equilibrate for 5 min. With rapid stirring, the reactor was then pressurized to 8.0 atm ethylene pressure, which was maintained during the course of the polymerization. After 50 min the reactor was vented to 1.0 atm ethylene pressure. The glass pressure vessel was then interfaced to a Schlenk line and all volatiles were removed, in vacuo. Air-free ^{1}H NMR (C_6D_6) analysis of the residue confirmed the formation of free ligand.

X-ray crystal structure determinations of (CF$_3$)H$_2$FI^2, and **(CF$_3$)FI^2-Ni$_2$**: Intensity data for **(CF$_3$)H$_2$FI^2** and **(CF$_3$)FI^2-Ni$_2$** were collected at −173 °C on a Bruker AXS APEXII diffractometer equipped with a CCD area detector by using graphite-monochromated $Mo_{K\alpha}$ [$\lambda = 0.7107$ Å, **(CF$_3$)H$_2$FI^2**] or $Cu_{K\alpha}$ [$\lambda = 1.5418$ Å, **(CF$_3$)FI^2-Ni$_2$**] radiation. All data were corrected for absorption by using an empirical correction. Structure solutions and refinements were obtained by using SIR-92[51] or SHELXS-97[52] with direct methods and were refined on F^2 with the use of full-matrix least-squares techniques. All aromatic hydrogen atoms were refined with a riding model. All non-hydrogen atoms were refined anisotropically and hydrogen atoms were either located in the difference map or were refined with a riding model. Crystallographic results are summarized in Table S1 of the Supporting Information. CCDC-869747 [for **(CF$_3$)H$_2$FI^2**], -869748 [for **2-CH$_3$**], and -869750 [for **(CF$_3$)FI^2-Ni$_2$**], contain the supplementary crystallographic data for this paper. These data can be obtained free of charge from The Cambridge Crystallographic Data Centre via www.ccdc.cam.ac.uk/data_request/cif.

Acknowledgements

Financial support from DOE (grant 86ER13511) and NSF (grant CHE-0809589) is gratefully acknowledged. We also acknowledge Albemarle Corporation for the generous gift of $B(C_6F_5)_3$. We thank Dr. C. Weiss, Ms. J. McInnis, and Mr. S. Wobser for helpful discussions.

[1] For recent reviews on olefin polymerization catalysis with bimetallic catalysts, see: a) M. Delferro, T. J. Marks, *Chem. Rev.* **2011**, *111*, 2450–2485; b) H. Li, T. J. Marks, *Proc. Natl. Acad. Sci. USA* **2006**, *103*, 15295–15302.

[2] a) N. Guo, C. L. Stern, T. J. Marks, *J. Am. Chem. Soc.* **2008**, *130*, 2246–2247; b) S. Amin, T. J. Marks, *J. Am. Chem. Soc.* **2007**, *129*, 2938–2953; c) S. Amin, T. J. Marks, *J. Am. Chem. Soc.* **2006**, *128*, 4506–4507; d) H. Li, L. Li, D. J. Schwartz, M. V. Metz, T. J. Marks, L. Liable-Sands, A. L. Rheingold, *J. Am. Chem. Soc.* **2005**, *127*, 14756–14768; e) H. Li, C. L. Stern, T. J. Marks, *Macromolecules* **2005**, *38*, 9015–9027; f) H. Li, L. Li, T. J. Marks, *Angew. Chem.* **2004**, *116*, 5045–5048; *Angew. Chem. Int. Ed.* **2004**, *43*, 4937–4940; g) N. Guo, L. Li, T. J. Marks, *J. Am. Chem. Soc.* **2004**, *126*, 6542–6543; h) H. Li, L. Li, T. J. Marks, L. Liable-Sands, A. L. Rheingold, *J. Am. Chem. Soc.* **2003**, *125*, 10788–10789; i) L. Li, M. V. Metz, H. Li, M.-C. Chen, T. J. Marks, L. Liable-Sands, A. L. Rheingold, *J. Am. Chem. Soc.* **2002**, *124*, 12725–12741.

[3] a) L. R. Gahan, S. J. Smith, A. Neves, G. Schenk, *Eur. J. Inorg. Chem.* **2009**, 2745–2758; b) X. Cao, S. V. Antonyuk, S. V. Seetharaman, L. J. Whitson, A. B. Taylor, S. P. Holloway, R. W. Strange, P. A. Doucette, J. S. Valentine, A. Tiwari, L. J. Hayward, S. Padua, J. A. Cohlberg, S. S. Hasnain, P. J. Hart, *J. Biol. Chem.* **2008**, *283*, 16169–16177; c) N. Mitić, S. J. Smith, A. Neves, L. W. Guddat, L. R. Gahan, G. Schenk, *Chem. Rev.* **2006**, *106*, 3338–3363; d) C. Belle, J. L. Pierre, *Eur. J. Inorg. Chem.* **2003**, 4137–4146; e) M. J. Jedrzejas, P. Setlow, *Chem. Rev.* **2001**, *101*, 607–618; f) T. C. Bruice, S. J. S. Benkovic, *Biochemistry* **2000**, *39*, 6267–6274; g) E. Jabri, M. B. Carr, R. P. Hausinger, P. A. Karplus, *Science* **1995**, *268*, 998–1004; h) V. K. Yachandra, K. Sauer, M. P. Klein, *Chem. Rev.* **1996**, *96*, 2927–2950.

[4] a) B. Bauer-Siebenlist, S. Decher, F. Meyer, *Chem. Eur. J.* **2005**, *11*, 5343–5352; b) J. P. Collman, R. Boulatov, C. J. Sunderland, L. Fu, *Chem. Rev.* **2004**, *104*, 561–588; c) R. Krishnan, J. K. Voo, C. G. Riordan, L. Zahkarov, A. L. Rheingold, *J. Am. Chem. Soc.* **2003**, *125*, 4422–4423; d) T. C. Bruice, *Acc. Chem. Res.* **2002**, *35*, 139–148; e) D. P. O'Brien, R. M. N. Entress, A. C. Matthew, S. W. O'Brien, A. Hopkinson, D. H. Williams, *J. Am. Chem. Soc.* **1999**, *121*, 5259–5265; f) R. E. Carazo-Salas, G. Guarguaglini, O. J. Gruss, A. Segref, E. Karsenti, L. W. Mattaj, *Nature* **1999**, *400*, 178–181; g) F. M. Menger, *Acc. Chem. Res.* **1993**, *26*, 206–212.

[5] a) H. Steinhagen, G. Helmchen, *Angew. Chem.* **1996**, *108*, 2489–2492; *Angew. Chem. Int. Ed. Engl.* **1996**, *35*, 2339–2342; b) D. E. Wilcox, *Chem. Rev.* **1996**, *96*, 2435–2458; c) N. Sträter, W. N. Lipscomb, T. Klabunde, B. Krebs, *Angew. Chem.* **1996**, *108*, 2158–2191; *Angew. Chem. Int. Ed. Engl* **1996**, *35*, 2024–2055.

[6] B. A. Rodriguez, M. Delferro, T. J. Marks, *J. Am. Chem. Soc.* **2009**, *131*, 5902–5919.

[7] A. Motta, I. L. Fragala', T. J. Marks, *J. Am. Chem. Soc.* **2009**, *131*, 3974–3984.

[8] a) A. W. Waltman, T. R. Younkin, R. H. Grubbs, *Organometallics* **2004**, *23*, 5121–5123; b) E. F. Connor, T. R. Younkin, J. I. Henderson, A. W. Waltman, R. H. Grubbs, *Chem. Commun.* **2003**, 2272–2273; c) T. R. Younkin, E. F. Connor, J. I. Henderson, S. K. Friedrich, R. H. Grubbs, D. A. Bansleben, *Science* **2000**, *287*, 460–462; d) C. Wang, S. Friedrich, T. R. Younkin, R. T. Li, R. H. Grubbs, D. A. Bansleben, M. W. Day, *Organometallics* **1998**, *17*, 3149–3151.

[9] a) H. Makio, H. Terao, A. Iwashita, T. Fujita, *Chem. Rev.* **2011**, *111*, 2363–2449; b) M. Mitani, R. Furuyama, J.-I. Mohri, J. Saito, S. Ishii, H. Terao, T. Nakano, H. Tanaka, T. Fujita, *J. Am. Chem. Soc.* **2003**, *125*, 4293–4305; c) S.-I. Ishii, R. Furuyama, N. Matsukawa, J. Saito, M. Mitani, H. Tanaka, T. Fujita, *Macromol. Rapid Commun.* **2003**, *24*, 452–456; d) M. Mitani, J.-I. Mohri, Y. Yoshida, J. Saito, S. Ishii, K. Tsuru, S. Matsui, R. Furuyama, T. Nakano, H. Tanaka, S.-I. Kojoh, T. Matsugi, N. Kashiwa, T. Fujita, *J. Am. Chem. Soc.* **2002**, *124*, 3327–3336.

[10] a) M. R. Salata, T. J. Marks, *Macromolecules* **2009**, *42*, 1920–1933; b) M. R. Salata, T. J. Marks, *J. Am. Chem. Soc.* **2008**, *130*, 12–13.

[11] a) D. Takeuchi, *Dalton Trans.* **2010**, *39*, 311–328; b) A. Nakamura, S. Ito, K. Nozaki, *Chem. Rev.* **2009**, *109*, 5215–5244; c) E. Y. X. Chen, *Chem. Rev.* **2009**, *109*, 5157–5214; d) G. J. Domski, J. M. Rose, G. W. Coates, A. D. Bolig, M. Brookhart, *Prog. Polym. Sci.* **2007**, *32*, 30–92; e) J. Zhang, X. Wang, G. X. Jin, *Coord. Chem. Rev.* **2006**, *250*, 95–109; f) J. Durand, B. Milani, *Coord. Chem. Rev.* **2006**, *250*, 542–560; g) V. C. Gibson, S. K. Spitzmesser, *Chem. Rev.* **2003**, *103*, 283–316; h) S. Mecking, *Coord. Chem. Rev.* **2000**, *203*, 325–351; i) S. D. Ittel, L. K. Johnson, M. Brookhart, *Chem. Rev.* **2000**, *100*, 1169–1204; j) L. S. Boffa, B. M. Novak, *Chem. Rev.* **2000**, *100*, 1479–1493; k) G. J. P. Britovsek, V. C. Gibson, D. F. Wass, *Angew. Chem.* **1999**, *111*, 448–468; *Angew. Chem. Int. Ed.* **1999**, *38*, 428–447.

[12] a) D. Guironnet, I. Goettker-Schnetmann, S. Mecking, *Macromolecules* **2009**, *42*, 8157–8164; b) D. Guironnet, T. Friedberger, S. Mecking, *Dalton Trans.* **2009**, 8929–8934; c) D. H. Camacho, Z. Guan, *Macromolecules* **2005**, *38*, 2544–2546; d) D. H. Camacho, E. V. Salo, J. W. Ziller, Z. Guan, *Angew. Chem.* **2004**, *116*, 1857–1861; *Angew. Chem. Int. Ed.* **2004**, *43*, 1821–1825; e) Z. Guan, *Chem. Eur. J.* **2002**, *8*, 3086–30902; f) S. Mecking, *Angew. Chem.* **2001**, *113*, 550–557; *Angew. Chem. Int. Ed.* **2001**, *40*, 534–540.

[13] a) B. M. Boardman, G. C. Bazan, *Acc. Chem. Res.* **2009**, *42*, 1597–1606; b) K. C. Gupta, A. K. Sutar, *Coord. Chem. Rev.* **2008**, *252*, 1420–1450; c) P. Kuhn, D. Semeril, D. Matt, M. J. Chetcuti, P. Lutz, *Dalton Trans.* **2007**, 515–528; d) F. Speiser, P. Braunstein, L. Saussine, *Acc. Chem. Res.* **2005**, *38*, 784–793; e) J. Heinicke, N. Peulecke, M. Koehler, M. He, W. Keim, *J. Organomet. Chem.* **2005**, *690*, 2449–2457; f) P. Braunstein, *J. Organomet. Chem.* **2004**, *689*, 3953–3967.

[14] a) C. S. Popeney, C. M. Levins, Z. Guan, *Organometallics* **2011**, *30*, 2432–2452; b) D.-P. Song, Y.-X. Wang, H.-L. Mu, B.-X. Li, Y.-S. Li, *Organometallics* **2011**, *30*, 925–934; c) M. Delferro, J. P. McInnis, T. J. Marks, *Organometallics* **2010**, *29*, 5040–5049; d) C. Chen, S. Luo, R. F. Jordan, *J. Am. Chem. Soc.* **2010**, *132*, 5273–5284; e) D. H. Camacho, Z. Guan, *Chem. Commun.* **2010**, *46*, 7879–7893; f) A. Berkefeld, H. M. Möller, S. Mecking, *Organometallics* **2009**, *28*, 4048–4055; g) A. Berkefeld, M. Drexler, H. M. Möller, S. Mecking, *J. Am. Chem. Soc.* **2009**, *131*, 12613–12622; h) S. Noda, A. Nakamura, T. Kochi, L. W. Chung, K. Morokuma, K. Nozaki, *J. Am. Chem. Soc.* **2009**, *131*, 14088–14100; i) C. Chen, S. Luo, R. F. Jordan, *J. Am. Chem. Soc.* **2008**, *130*, 12892–12893; j) P. Wehrmann, S. Mecking, *Organometallics* **2008**, *27*, 1399–1408; k) D. H. Leung, J. W. Ziller, Z. Guan, *J. Am. Chem. Soc.* **2008**, *130*, 7538–7539; l) B. Korthals, I. Goettker-Schnetmann, S. Mecking, *Organometallics* **2007**, *26*, 1311–1316; m) C. S. Popeney, D. H. Camacho, Z. Guan, *J. Am. Chem. Soc.* **2007**, *129*, 10062–10063; n) S. Luo, R. F. Jordan, *J. Am. Chem. Soc.* **2006**, *128*, 12072–12073; o) P. Wehrmann, S. Mecking, *Macromolecules* **2006**, *39*, 5963–5964; p) S. R. Foley, R. A. Stockland, H. Shen, R. F. Jordan, *J. Am. Chem. Soc.* **2003**, *125*, 4350–4361; q) E. F. Connor, T. R. Younkin, J. I. Henderson, S. Hwang, R. H. Grubbs, W. P. Roberts, J. J. Litzau, *J. Polym. Sci. Part A* **2002**, *40*, 2842–2854.

[15] a) M. D. Leatherman, M. Brookhart, *Macromolecules* **2001**, *34*, 2748–2750; b) D. P. Gates, S. A. Svejda, E. Onate, C. M. Killian, L. K. Johnson, P. S. White, M. Brookhart, *Macromolecules* **2000**, *33*, 2320–2334; c) S. Mecking, L. K. Johnson, L. Wang, M. Brookhart, *J. Am. Chem. Soc.* **1998**, *120*, 888–899; d) L. K. Johnson, S. Mecking, M. Brookhart, *J. Am. Chem. Soc.* **1996**, *118*, 267–268; e) C. M. Killian, D. J. Tempel, L. K. Johnson, M. Brookhart, *J. Am. Chem. Soc.* **1996**, *118*, 11664–11665; f) L. K. Johnson, C. M. Killian, M. Brookhart, *J. Am. Chem. Soc.* **1995**, *117*, 6414–6415.

[16] a) E. F. McCord, S. J. McLain, L. T. J. Nelson, S. D. Ittel, D. Tempel, C. M. Killian, L. K. Johnson, M. Brookhart, *Macromolecules* **2007**, *40*, 410–420; b) L. Zhang, M. Brookhart, P. S. White, *Organometallics* **2006**, *25*, 1868–1874; c) A. E. Cherian, J. M. Rose, E. B. Lobkovsky, G. W. Coates, *J. Am. Chem. Soc.* **2005**, *127*, 13770–13771; d) W. Liu, M. Brookhart, *Organometallics* **2004**, *23*, 6099–6107; e) M. D. Leatherman, S. A. Svejda, L. K. Johnson, M. Brookhart, *J. Am. Chem. Soc.* **2003**, *125*, 3068–3081; f) A. C. Gottfried, M. Brookhart, *Macromolecules* **2003**, *36*, 3085–3100; g) L. H. Shultz, D. J. Tempel, M. Brookhart, *J. Am. Chem. Soc.* **2001**, *123*, 11539–11555; h) L. H. Shultz, M. Brookhart, *Organometallics* **2001**, *20*, 3975–3982; i) A. C. Gottfried, M. Brookhart, *Macromolecules* **2001**, *34*, 1140–1142; j) D. J. Tempel, L. K. Johnson, R. L. Huff, P. S. White, M. Brookhart, *J. Am. Chem. Soc.* **2000**, *122*, 6686–6700; k) S. A. Svejda, L. K. Johnson, M. Brookhart, *J. Am. Chem. Soc.* **1999**, *121*, 10634–10635; l) Z. Guan, P. M. Cotts, E. F. McCord, S. J. McLain, *Science* **1999**, *283*, 2059–2062.

[17] M. P. Weberski, Jr., C. Chen, M. Delferro, C. Zuccaccia, A. Macchioni, T. J. Marks, *Organometallics* **2012**, *31*, 3773–3789.

[18] a) H.-J. Schneider, *Chem. Sci.* **2012**, *3*, 1381–1394; b) E. D'Oria, J. J. Novoa, *CrystEngComm* **2008**, *10*, 423–436; c) K. Reichenbacher, H. I. Suss, J. Hulliger, *Chem. Soc. Rev.* **2005**, *34*, 22–30; d) I. Hyla-Kryspin, G. Haufe, S. Grimme, *Chem. Eur. J.* **2004**, *10*, 3411–3422; e) G. R. Desiraju, *Acc. Chem. Res.* **2002**, *35*, 565–573; f) J. Parsch, J. W. Engels, *J. Am. Chem. Soc.* **2002**, *124*, 5664–5672; g) L. Shimoni, H. L. Carrell, J. P. Glusker, M. M. Coombs, *J. Am. Chem. Soc.* **1994**, *116*, 8162–8168.

[19] a) L.-C. So, C.-C. Liu, M. C. W. Chan, J. C. Y. Lo, K.-H. Sze, N. Zhu, *Chem. Eur. J.* **2012**, *18*, 565–573; b) H. M. Möller, M. C. Baier, S. Mecking, E. P. Talsi, K. P. Bryliakov, *Chem. Eur. J.* **2012**, *18*, 848–856; c) M. C. W. Chan, *Chem. Asian J.* **2008**, *3*, 18–27; d) M. C. W. Chan, S. C. F. Kui, J. M. Cole, G. J. McIntyre, S. Matsui, N. Zhu, K.-H. Tam, *Chem. Eur. J.* **2006**, *12*, 2607–2619; e) S. C. F. Kui, N. Zhu, M. C. W. Chan, *Angew. Chem.* **2003**, *115*, 1666–1670; *Angew. Chem. Int. Ed.* **2003**, *42*, 1628–1632.

[20] B. A. Rodriguez, M. Delferro, T. J. Marks, *Organometallics* **2008**, *27*, 2166–2168.

[21] T. Glaser, I. Liratzis, *Synlett* **2004**, 735–737.

[22] D. Meinhard, M. Wegner, G. Kipiani, A. Hearley, P. Reuter, S. Fischer, O. Marti, B. Rieger, *J. Am. Chem. Soc.* **2007**, *129*, 9182–9191.

[23] The half-condensation of **$(CH_3)H_2FI^2$** has been structurally characterized by X-ray diffraction. Please see the Supporting Information.

[24] Solution of **$(CF_3)H_2FI^2$** is less susceptible to hydrolysis than **$(CH_3)H_2FI^2$**.

[25] a) E. Malamidou-Xenikaki, S. Spyroudis, M. Tsanakopoulou, H. Krautscheid, *J. Org. Chem.* **2007**, *72*, 502–508; b) J. J. Charette, H. E. De, *J. Org. Chem.* **1979**, *44*, 2256–2262.

[26] J. L. Burdett, M. T. Rogers, *J. Am. Chem. Soc.* **1964**, *86*, 2105–2109.

[27] a) H. Tanak, *J. Phys. Chem. A* **2011**, *115*, 13865–13876; b) S. Guieu, A. K. Crane, M. J. MacLachlan, *Chem. Commun.* **2011**, *47*, 1169–1171; c) D. Nedeltcheva, L. Antonov, *J. Phys. Org. Chem.* **2009**, *22*, 274–281; d) T. Dziembowska, M. Szafran, A. Katrusiak, Z. Rozwadowski, *J. Mol. Struct.* **2009**, *929*, 32–42; e) S. H. Alarcon, A. C. Olivieri, D. Sanz, R. M. Claramunt, J. Elguero, *J. Mol. Struct.* **2004**, *705*, 1–9; f) A. Hetenyi, Z. Szakonyi, K. D. Klika, K. Pihlaja, F. Fueloep, *J. Org. Chem.* **2003**, *68*, 2175–2182.

[28] The presence of coordinated THF molecules was confirmed by ^{1}H NMR spectrscopy.

[29] H. F. Klein, H. H. Karsch, *Chem. Ber.* **1972**, *105*, 2628–2636.

[30] A. Filarowski, A. Koll, L. Sobczyk, *Curr. Org. Chem.* **2009**, *13*, 172–193.

[31] a) G. M. Battle, F. H. Allen, *J. Chem. Educ.* **2012**, *89*, 38–44; b) R. A. Sykes, P. McCabe, F. H. Allen, G. M. Battle, I. J. Bruno, P. A. Wood, *J. Appl. Crystallogr.* **2011**, *44*, 882–886; c) F. H. Allen, R. Taylor, *Chem. Soc. Rev.* **2004**, *33*, 463–475.

[32] The average distances found in the Cambridge Crystallographic Data Centre (CDC, Feb. 2012) are: Ni–O_{phenol} = 1.911; Ni–N_{imine} = 1.981; Ni–C_{methyl} = 1.935; Ni–$P_{phosphine}$ = 2.198; C=N_{imine} = 1.295; C–O_{phenol} = 1.299 Å.
[33] a) Q. Chen, J. Yu, J. Huang, *Organometallics* **2007**, *26*, 617–625; b) D. Zhang, G.-X. Jin, *Inorg. Chem. Commun.* **2006**, *9*, 1322–1325; c) S. Sujith, D. J. Joe, S. J. Na, Y. Park, C. H. Choi, B. Y. Lee, *Macromolecules* **2005**, *38*, 10027–10033; d) T. Hu, L. Tang, X. Li, Y. Li, N. Hu, *Organometallics* **2005**, *24*, 2628–2632; e) D. Zhang, G. Jin, *Organometallics* **2003**, *22*, 2851–2584; f) K. Kurtev, A. Tomov, *J. Mol. Catal.* **1994**, *88*, 141–150.
[34] A. Bondi, *J. Phys. Chem.* **1964**, *68*, 441–451.
[35] a) J. C. Jenkins, M. Brookhart, *Organometallics* **2003**, *22*, 250–256; b) W. Liu, D. G. Ray, P. L. Rinaldi, *Macromolecules* **1999**, *32*, 3817–3819; c) M. De Pooter, P. B. Smith, K. K. Dohrer, K. F. Bennett, M. D. Meadows, C. G. Smith, H. P. Schouwenaars, R. A. Geerards, *J. Appl. Polym. Sci.* **1991**, *42*, 399–408.
[36] See the Supporting Information.
[37] a) N. Osamu, M. Hideki, S. Ryosuke, K. Toyoji, S. Toshifumi, *J. Polym. Sci. Part A* **2008**, *46*, 7411–7418; b) T. Hasan, T. Ikeda, T. Shiono, *Macromolecules* **2004**, *37*, 8503–8509.
[38] a) A. Berkefeld, S. Mecking, *J. Am. Chem. Soc.* **2009**, *131*, 1565–1574; b) J. C. Jenkins, M. Brookhart, *J. Am. Chem. Soc.* **2004**, *126*, 5827–5842.
[39] a) B. L. Durfey, T. M. Gilbert, *Inorg. Chem.* **2011**, *50*, 7871–7879; b) G. C. Welch, T. Holtrichter-Roessmann, D. W. Stephan, *Inorg. Chem.* **2008**, *47*, 1904–1906; c) P. A. Chase, M. Parvez, W. E. Piers, *Acta Crystallogr. E* **2006**, *62*, o5181–o5183; d) B. Y. Lee, X. Bu, G. C. Bazan, *Organometallics* **2001**, *20*, 5425–5431; e) G. S. Hair, R. A. Jones, A. H. Cowley, V. Lynch, *Organometallics* **2001**, *20*, 177–181.
[40] W. A. Henderson, C. A. Streuli, *J. Am. Chem. Soc.* **1960**, *82*, 5791–5794.
[41] F.-G. Fontaine, M.-A. Dubois, D. Zargarian, *Organometallics* **2001**, *20*, 5156–5161.
[42] M. R. Radlauer, M. W. Day, T. Agapie, *J. Am. Chem. Soc.* **2012**, *134*, 1478–1481.
[43] For DFT calculations of the agostic C–H···Ni interaction, see a) M. E. Evans, T. Li, W. D. Jones, *J. Am. Chem. Soc.* **2010**, *132*, 16278–16284; b) M. P. Mitoraj, A. Michalak, T. Ziegler, *Organometallics* **2009**, *28*, 3727–3733; c) T. S. Thakur, G. R. Desiraju, *J. Mol. Struc. Theochem.* **2007**, *810*, 143–154; d) Y. Liu, M. G. B. Drew, Y. Liu, *J. Mol. Struc. Theochem.* **2007**, *821*, 30–41; e) S. Collins, T. Ziegler, *Organometallics* **2007**, *26*, 6612–6623; f) E. Kogut, A. Zeller, T. H. Warren, T. Strassner, *J. Am. Chem. Soc.* **2004**, *126*, 11984–11994; g) T. Tomita, T. Takahama, M. Sugimoto, S. Sakaki, *Organometallics* **2002**, *21*, 4138–4146; h) L. Fan, A. Krzywicki, A. Somogyvari, T. Ziegler, *Inorg. Chem.* **1994**, *33*, 5287–5294; i) N. Koga, S. Obara, K. Kitaura, K. Morokuma, *J. Am. Chem. Soc.* **1985**, *107*, 7109–7116.
[44] a) P. H. M. Budzelaar, N. N. P. Moonen, R. de Gelder, J. M. M. Smits, A. W. Gal, *Eur. J. Inorg. Chem.* **2000**, 753–769; b) D. B. Brown, M. Cripps, B. F. G. Johnson, C. M. Martin, D. Braga, F. Grepioni, *Chem. Commun.* **1996**, 1425–1426; c) M. Pasquali, C. Floriani, A. Gaetani-Manfredotti, A. Chiesi-Villa, *J. Am. Chem. Soc.* **1978**, *100*, 4918–4919.
[45] M. D. Walter, R. A. Moorhouse, S. A. Urbin, P. S. White, M. Brookhart, *J. Am. Chem. Soc.* **2009**, *131*, 9055–9069.
[46] See the Supporting Information.
[47] M. Peuckert, W. Keim, *Organometallics* **1983**, *2*, 594–597.
[48] B. Akermark, J. Martin, J.-E. Nystrom, S. Stromberg, M. Svensson, K. Zetterberg, M. Zuber, *Organometallics* **1998**, *17*, 5367–5373.
[49] a) L. Lavanant, A.-S. Rodrigues, E. Kirillov, J.-F. Carpentier, R. F. Jordan, *Organometallics* **2008**, *27*, 2107–2117; b) N. A. Cooley, S. M. Green, D. F. Wass, K. Heslop, A. G. Orpen, P. G. Pringle, *Organometallics* **2001**, *20*, 4769–4771.
[50] The GPC traces of the polyethylenes obtained from the in situ reaction of **$(CF_3)H_2FI^2$**/Ni$(COD)_2$ and the high molecular weight polyethylene fraction that grows in as polymerization times are increased where **$(CF_3)FI^2$-Ni_2** is the catalyst, do not overlap. Presumably this is due to difficulties in matching exact polymerization conditions. Nevertheless, the observation that the in situ combination of **$(CF_3)H_2FI^2$**/Ni$(COD)_2$ produces high M_w polyethylene indicates the "non-innocent" role Ni$(COD)_2$ plays in these polymerizations.
[51] A. Altomere, M. C. Burla, G. Camilla, G. Cascarano, C. Giacovazzo, A. Gualiardi, G. Polidori, *J. Appl. Crystallogr.* **1994**, *27*, 435.
[52] G. Sheldrick, *Acta Crystallogr. A* **2008**, *64*, 112–122.

Received: March 2, 2012
Published online: ■■ ▮▮, 0000

Ni-ce cats: Two neutrally charged bimetallic phenoxyiminato Ni^{II} ethylene polymerization catalysts are reported. Significant Ni···Ni cooperative effects are evidenced by increased product polyethylene branching in ethylene homopolymerizations and by enhanced norbornene co-monomer incorporation selectivity in ethylene–norbornene copolymerization than monometallic controls.

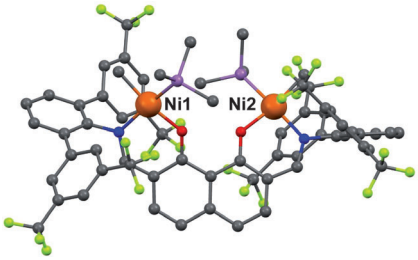

Homogeneous Catalysis

M. P. Weberski, Jr., C. Chen, M. Delferro, T. J. Marks* ..* ▮▮▮▮–▮▮▮▮

Ligand Steric and Fluoroalkyl Substituent Effects on Enchainment Cooperativity and Stability in Bimetallic Nickel(II) Polymerization Catalysts